

Comprehensive analysis of *Verticillium nonalfalfae* *in silico* secretome uncovers putative effector proteins expressed during hop invasion

1 **Kristina Marton¹, Marko Flajšman¹, Sebastjan Radišek², Katarina Košmelj¹, Jernej Jakše¹,**
2 **Branka Javornik¹, Sabina Berne^{1*}**

3 ¹Department of Agronomy, Biotechnical Faculty, University of Ljubljana, Ljubljana, Slovenia

4 ²Slovenian Institute of Hop Research and Brewing, Žalec, Slovenia

5 *** Correspondence:**

6 Sabina Berne

7 sabina.berne@bf.uni-lj.si

8 **Abstract**

9 Background: The vascular plant pathogen *Verticillium nonalfalfae* causes Verticillium wilt in several
10 important crops. *VnaSSP4.2* was recently discovered as a *V. nonalfalfae* virulence effector protein in
11 the xylem sap of infected hop. Here, we expanded our search for candidate secreted effector proteins
12 (CSEPs) in the *V. nonalfalfae* predicted secretome using a bioinformatic pipeline built on *V.*
13 *nonalfalfae* genome data, RNA-Seq and proteomic studies of the interaction with hop.

14 Results: The secretome, rich in carbohydrate active enzymes, proteases, redox proteins and proteins
15 involved in secondary metabolism, cellular processing and signaling, includes 263 CSEPs. Several
16 homologs of known fungal effectors (LysM, NLPs, Hce2, Cerato-platanins, Cyanovirin-N lectins,
17 hydrophobins and CFEM domain containing proteins) and avirulence determinants in the PHI
18 database (Avr-Pita1 and MgSM1) were found. The majority of CSEPs were non-annotated and were

19 narrowed down to 44 top priority candidates based on their likelihood of being effectors. These were
20 examined by spatio-temporal gene expression profiling of infected hop. Among the highest *in planta*
21 expressed CSEPs, five deletion mutants were tested in pathogenicity assays. A deletion mutant of
22 *VnaUn.279*, a lethal pathotype specific gene with sequence similarity to SAM-dependent
23 methyltransferase (*LaeA*), had lower infectivity and showed highly reduced virulence, but no
24 changes in morphology, fungal growth or conidiation were observed.

25 Conclusions: Several putative secreted effector proteins that probably contribute to *V. nonalfalfae*
26 colonization of hop were identified in this study. Among them, *LaeA* gene homolog was found to act
27 as a potential novel virulence effector of *V. nonalfalfae*. The combined results will serve for future
28 characterization of *V. nonalfalfae* effectors, which will advance our understanding of *Verticillium*
29 wilt disease.

30 **Keywords:** *Verticillium*, hop, plant-pathogen interaction, effector, secretome, ATMT, virulence,
31 **LaeA**

32 **1 Background**

33 Soil-born vascular plant pathogens, members of the *Verticillium* genus [1], cause *Verticillium* wilt in
34 several economically important crops, including tomato, potato, cotton, hop, sunflower and woody
35 perennials [2,3]. Studies of *Verticillium* – host interactions and disease processes, particular those
36 caused by *V. dahliae*, have significantly contributed to the understanding of *Verticillium* spp.
37 pathogenicity, although more research is needed for successful implementation of *Verticillium* wilt
38 disease control [4–6].

39 Plant-colonizing fungi secrete a number of effectors, consisting among others of hydrolytic enzymes,
40 toxic proteins and small molecules, to alter the host cell structure and function, thereby facilitating

41 infection and/or triggering defense responses [7]. The assortment of effector molecules is complex
42 and highly dynamic, reflecting the fungal pathogenic lifestyle [8] and leading to pathogen
43 perpetuation and development of disease. Research into plant-pathogen interactions has significantly
44 advanced, with an increasing number of sequenced microbial genomes, which have enabled
45 computational prediction of effectors and subsequent functional and structural characterization of
46 selected candidates. However, the prediction of fungal effectors, mainly small secreted proteins,
47 which typically lack conserved sequence motifs and structural folds, is challenging and largely based
48 on broad criteria, such as the presence of a secretion signal, no similarities with other protein
49 domains, relatively small size, high cysteine content and species-specificity [8–10]. Using these
50 features to mine predicted secretomes for candidate effectors has been valuable, but has not produced
51 a one-size-fits-all solution [11]. Various approaches that combine several bioinformatics tools and
52 also consider features such as diversifying selection, genome location and expression *in planta* [12–
53 15], have had mixed outcomes. The EffectorP application has recently been presented as the first
54 machine learning approach to predicting fungal effectors with over 80% sensitivity and specificity
55 [16].

56 The genome sequences of five *Verticillium* species (*V. dahliae*, *V. alfalfae*, *V. tricorpus*, *V.*
57 *longisporum* and *V. nonalfalfae*) and their strains have been published [17–22], providing a wealth of
58 genomic information for various studies. Klosterman et al. [17] queried *V. dahliae* (strain VdLs.17)
59 and *V. alfalfae* (strain VaMs.102) genomes for potential effectors and other secreted proteins based
60 on subcellular localization and the presence of signal peptide. A similar number of secreted proteins
61 was found in both genomes (780 and 759 for *V. dahliae* and *V. alfalfae*, respectively), and
62 comparable to other fungi. These secretomes were further examined for effector candidates,
63 obtaining 127 for *V. dahliae* and 119 for *V. alfalfae* proteins, based on the assumption that fungal
64 effectors are small cysteine-rich proteins (SSCPs) with fewer than 400 amino acids and more than

65 four cysteine residues. Siedl et al. [19] later re-examined the secretomes of two *V. dahliae* strains
66 (VdLs.17 and JR2) and *V. alfalfae* (VaMs.102), and predicted a higher number of secreted proteins
67 and smaller number of SSCPs, due to improved gene annotation and restricted criteria for SSCPs.
68 Interestingly, in their comparison of highly pathogenic *Verticillium* species with saprophytic and
69 weak pathogen *V. tricorpus*, a similar content of the secretome (cca 8.5%) in their respective
70 proteomes was obtained. Orthologs of known effectors of *F. oxysporum*, *C. fulvum* or oomycete
71 *Phytophthora infestans* were not found in *V. dahliae* and *V. alfalfae* genomes [17], except for *C.*
72 *fulvum* LysM effector Ecp6 [23] (7 and 6 genes in *V. dahliae* and *V. alfalfae*, respectively) and *C.*
73 *fulvum* virulence factor Ecp2 [24]. Several LysM effectors, widespread fungal proteins recognized by
74 the LysM domain, have also been characterized as suppressors of PTI (PAMP-triggered immunity)
75 through their chitin binding ability [25–28]. Reexamination of *Verticillium* LysM effectors has
76 corroborated only three LysM effectors as core proteins in the genomes of *V. dahliae* strains with a
77 function other than fungal pathogenicity, and one strain specific (VdLs.17) virulence associated
78 LysM protein [18,27]. An increase in NLP (necrosis and ethylene-inducing protein (NEP-1)-like
79 proteins) gene homologs has also been found among secreted proteins in *Verticillium* genomes (8 and
80 7 in *V. dahliae* and *V. alfalfae*, respectively) [17,19]. Zhou et al. [29] and Santhanam et al. [30]
81 showed that only two of them displayed cytotoxic activity in tomato, cotton, *Arabidopsis* and
82 *Nicotiana benthamiana*, while reduced virulence has been demonstrated for the deletion mutant of
83 *VdNLP1* and *VdNLP2* in tomato and *Arabidopsis*.

84 Although numerous secreted proteins with unknown function or sequence similarity have been
85 reported for *Verticillium* spp, only a handful have been characterized. Virulence effector Ave1 is a
86 134 aa long secreted protein with 4 conserved cysteines and an Expansin-like EG45 domain,
87 discovered by comparative genomics in *V. dahliae* race 1 strains [31]. Ave1 recognition by tomato
88 receptor-like protein Ve1 triggered immune signaling pathways leading to resistance to *V. dahliae*

89 race 1 strains [32,33]. The other reported *V. dahliae* effector protein, PevD1, induced a
90 hypersensitive response in tobacco [34,35] and triggered innate immunity in cotton plants, as
91 demonstrated by upregulation of defense-related genes, metabolic substance deposition and cell wall
92 modifications [36]. Zhang et al. [37] recently characterized a novel effector protein, VdSCP7, as a
93 host nucleus targeting protein, which induced a plant immune response and altered the plant's
94 susceptibility to fungal and oomycete pathogens.

95 In addition to *V. dahliae* effectors, a small secreted protein, VnaSSP4.2, with an important role in
96 fungal virulence, has been discovered in xylem sap during *V. nonalfalfae* infection of hops [38]. *V.*
97 *nonalfalfae* is another pathogenic species of the genus *Verticillium*, although with a narrower host
98 range than *V. dahlia* [1]. However, it causes Verticillium wilt and plant death in several important
99 crops [4]. The occurrence of different virulent strains has been well documented in hop (*Humulus*
100 *lupulus* L.), in which two pathotypes of *V. nonalfalfae* with different aggressiveness have been
101 isolated, causing mild (fluctuating) and lethal (progressive) disease forms [39–43]. The disease is
102 demonstrated by plant wilting, foliar chlorosis and necrosis, vascular browning and rapid plant
103 withering and dieback in the lethal disease form [43]. Sporadic outbreaks of the *V. nonalfalfae* lethal
104 pathotype in European hop gardens are of major concern, since there is no effective disease control
105 except host resistance and strict phytosanitary measures. Despite the high economic losses caused by
106 the lethal Verticillium wilt, the development of highly aggressive *V. nonalfalfae* pathotypes, as well
107 as the genetics of hop resistance, remains enigmatic.

108 In the present study, a comprehensive biological database was generated using data from recently
109 sequenced *V. nonalfalfae* genomes [22], transcriptomic and proteomic research of fungal growth on
110 xylem stimulating medium [44] and RNA-seq studies of *V. nonalfalfae* – hop interactions [45]. A
111 customized bioinformatics platform was used to set up a pipeline for prediction and characterization
112 of the *V. nonalfalfae* secretome and select the best candidate secreted effector proteins (CSEPs) for

113 functional studies. From a total of 263 CSEPs in the final dataset, the gene expression of the 44
114 highest ranking CSEPs was assessed by spatio-temporal RT-qPCR profiling of infected hop.
115 Furthermore, deletion mutants of five selected CSEPs were analyzed in pathogenicity assays, with
116 one of them exhibiting reduced virulence on hop plants. Our findings should assist further
117 characterization of *V. nonalfalfae* effectors in an attempt to understand the molecular mechanisms of
118 Verticillium wilt disease.

119 2 Results

120 2.1 The *V. nonalfalfae* *in silico* secretome is rich in carbohydrate-active enzymes, proteases 121 and candidate secreted effector proteins (CSEPs)

122 The *V. nonalfalfae* genome comprises 9,269 predicted protein-encoding genes. Among these putative
123 proteins, 944 are classically secreted proteins with signal peptide and no more than one
124 transmembrane domain, representing 10.2% of the *V. nonalfalfae* predicted proteome (Figure 1 and
125 Table S1). The accuracy of prediction was evaluated by comparing this dataset to a set of 91 unique
126 sequences obtained by proteomic analysis (2D-DIGE) of *V. nonalfalfae* proteins secreted in xylem
127 simulating medium [44], resulting in a 81.3% match (Table S1). Using TMHMM and Phobius [46]
128 for transmembrane (TM) domain prediction, 801 proteins without a TM domain and 161 proteins
129 harboring one TM domain were determined (Table S1). Based on subcellular localization predictions,
130 709 extracellular proteins ('extr' > 17) were acquired with WoLF PSORT [47], 450 proteins residing
131 in the apoplast were determined with ApoplastP [48], while Localizer [49] identified 52 proteins
132 harboring a chloroplast targeting signal and 12 proteins with a signal sequence for localization in
133 mitochondria (Table S1).

134 After similarity searches to known proteins in various databases, hypothetical functions were
135 assigned to 727 (77%) putatively secreted *V. nonalfalfae* proteins. A superfamily annotation scheme

136 [50] was used to classify the *V. nonalfalfae* secretome into seven functional groups (Figure 2). In the
137 'Metabolism' group, pectin lyase-like proteins and proteins with a cellulose-binding domain were
138 over-represented within the 'Polysaccharide metabolism and transport' category, while
139 (trans)glycosidases and six-hairpin glycosidases were predominant in the 'Carbohydrate metabolism
140 and transport' category. Other abundant proteins in the 'Metabolism' group were reductases and
141 heme-dependent peroxidases in the 'Redox' category, Concavalin A-like lectins/glucanases in the
142 'Secondary metabolism' category and 'Transferases'. The major constituents of the 'Intracellular
143 processes' group were 'Proteases' (especially acid proteases, Zn-dependent exopeptidases, subtilisin-
144 like proteases and metalloproteases), cupredoxins in the 'Ion metabolism and transport' category and
145 phospholipases in the 'Phospholipid metabolism and transport' category. Proteins involved in 'Cell
146 adhesion' were over-represented within 'Extracellular processes', while most proteins in the
147 'Information' group classified into the 'DNA replication/repair' category. In the 'General' group, FAD-
148 binding/transporter-associated domain-like proteins and proteins with a FAD/NAD(P)-binding
149 domain were major constituents in the 'Small molecule binding' category. Analysis of the EuKaryotic
150 Orthologous Groups (KOG) (Table S2) revealed a high number of proteins in the 'Cellular processing
151 and signaling' category, associated with posttranslational modification, protein turnover, chaperones
152 and signal transduction mechanisms, as well as cell wall/membrane/envelope biogenesis and
153 intracellular trafficking, secretion, and vesicular transport, while the protein composition of the
154 'Metabolism' category mirrored that of the Superfamily.

155 Since 'Carbohydrate metabolic process' and 'Peptidase activity' were overrepresented terms after
156 Blast2GO analysis of the *V. nonalfalfae* secretome (Figure S1), they were investigated more
157 thoroughly. Almost one third of the putative *V. nonalfalfae* secretome was CAZymes, of which 255
158 were expressed *in planta* and distributed as follows: glycoside hydrolases (129 GH), carbohydrate
159 esterases (47 CE), redox enzymes that act in conjunction with CAZymes (49 AA; proteins with

160 auxiliary activities), proteins with carbohydrate-binding modules (32 CBM), polysaccharide lyases
161 (25 PL), and glycosyltransferases (4 GT). This repertoire of CAZymes was compared to other plant
162 pathogenic *Verticillium* species (Figure 3A) and it was demonstrated that *V. nonalfalfae* had
163 statistically more putative secreted CEs than *V. alfalfae*, in particular those involved in deacetylation
164 of xylans and xylo-oligosaccharides. Moreover, the *V. nonalfalfae* secretome consisted of more
165 putative secreted GHs than *V. dahliae* with major differences found in the GH3 group consisting
166 primarily of stereochemistry-retaining β -glucosidases [51], the GH5 group of enzymes acting on β -
167 linked oligo- and polysaccharides, and glycoconjugates [52], and the GH43 group of enzymes for the
168 debranching and degradation of hemicellulose and pectin polymers [53]. In addition, the *V.*
169 *nonalfalfae* secretome was enriched in putative secreted proteins with CBMs, when compared to *V.*
170 *alfalfae*, *V. longisporum* and *V. dahlia*. This was largely due to cellulose-binding module CBM1
171 attached to various enzymes from families CE1, CE5, CE15, GH5, GH6, GH7, GH10, GH11, GH12,
172 GH45, GH74, PL1, PL3 and AA9, and to some extent due to chitin-binding module CBM50 found in
173 LysM effector proteins and subgroup C chitinases [54].

174 Similarity searching of *V. nonalfalfae* putative secreted proteins against peptidases in the *MEROPS*
175 database revealed 12 *in planta* expressed aspartic peptidases, 2 cysteine peptidases, 27
176 metallopeptidases, 44 serine peptidases and 1 threonine peptidase. The highest representation of *V.*
177 *nonalfalfae* putative secreted peptidases was in the M14A (carboxypeptidase A1), S08A (subtilisin
178 Carlsberg) and A01A (pepsin A) subfamilies (Table S3). Comparison of putative secreted peptidases
179 between plant pathogenic *Verticillium* species (Figure 3B) revealed a similar distribution of
180 peptidases among *V. nonalfalfae*, *V. alfalfae* and *V. longisporum*, while *V. dahliae* had a statistically
181 different distribution of metallopeptidases, cysteine and serine peptidases. Other enzymatic activities
182 of putatively secreted *V. nonalfalfae* proteins according to the KEGG analysis can be found in Table
183 S4.

184 Querying *Verticillium in silico* secretomes for small secreted proteins (SSPs) of less than 300 aa and
185 small secreted cysteine rich (SSCPs) proteins with more than 5% cysteine content and at least 4 Cys
186 residues [55] showed 5-10% lower abundance of SSPs and 2-3% fewer SSCPs in the *V. nonalfalfae*
187 secretome than in the secretomes of other plant pathogenic *Verticillium* species (Figure 3C). Since
188 small secreted proteins are the least characterized portion of fungal secretomes and many have been
189 shown to act as effectors, our secretome analysis further focused on filtering secreted proteins for
190 expression *in planta* to identify CSEPs relevant to *V. nonalfalfae* infection of hop. Genome-wide
191 transcriptome analysis of the *V. nonalfalfae* interaction with hop [45] revealed that 766 (81%)
192 transcripts in the *V. nonalfalfae in silico* secretome were expressed in infected hop samples. They
193 showed distinct expression patterns related to different stages of infection (6, 12, 18 and 30 dpi), hop
194 cultivar (susceptible 'Celeia' or resistant 'Wye Target') and plant tissue (roots or shoots) (Figure S2).
195 From this dataset, all CAZymes except CBMs were omitted from further analysis, resulting in 529
196 putatively secreted *in planta* expressed proteins (Figure 1), of which 308 had sequence similarity to
197 PFAM domains (Table S5). These included, among others, effector-specific PFAM domains, such as
198 LysM effectors [27], Necrosis inducing proteins (NPP1) [56], Hce2 (Homologs of *Cladosporium*
199 *fulvum* Ecp2 effector) effector proteins [57], Cerato-platanins [58], Cyanovirin-N lectins [59],
200 hydrophobins [60] and CFEM (Common in Fungal Extracellular Membranes) domain containing
201 proteins [61]. Our final dataset of CSEPs comprised a total of 263 proteins without functional PFAM
202 domains, and proteins bearing known effector-specific PFAM domains, representing 2.8% of the
203 putative proteome. Among them, we determined also 3 CSEPs with a nuclear localization signal
204 (NLS), implying their activity in the plant nucleus, 3 CSEPs specific to the lethal strain of *V.*
205 *nonalfalfae* and 69 probable effector proteins (Table S6) as predicted by EffectorP [16]. Similarity
206 searching of CSEPs to experimentally verified pathogenicity, virulence and effector genes from
207 fungal, oomycete and bacterial pathogens in the Pathogen-host interaction (PHI) database [62]

208 revealed proteins matching AVR effectors (5 hits) and known effector proteins displaying reduced
209 virulence (11 hits) or unaffected pathogenicity (4 hits) (Table S6).

210 **2.2 *V. nonalfalfae* CSEPs display distinct gene expression profiles during infection of hop**

211 Establishing successful colonization of a host plant requires effective and timely delivery of the
212 fungal pathogen's effectors. Using quantitative real-time PCR, the expression of the 44 top-priority
213 CSEPs selected according to their likelihood of being effectors (see Methods for selection criteria),
214 was investigated in root and shoot samples of *Verticillium* wilt susceptible ('Celeia') and resistant
215 ('Wye Target') hop at 6, 12 and 18 days after inoculation with *V. nonalfalfae*. In a preliminary
216 experiment, the average expression of the selected CSEPs in pooled root samples at different time
217 points was examined (Table S7). The three highest expressed CSEPs that were also selected by
218 Effector P prediction, and two lethal pathotype specific CSEPs, were then profiled using biological
219 replicates (Figure 4). We included the *VnaSSP4.2* gene, encoding a small secreted protein, in the
220 gene expression analysis as a positive control for virulence-associated *V. nonalfalfae* effector [38].

221 The expression levels of genes *Vna5.694*, *Vna7.443* and *Vna8.691* were greater in the roots than in
222 the shoots of both hop varieties. Gene expression of *Vna5.694* (Figure 4A), encoding a small (81 aa)
223 secreted cysteine-rich protein of unknown function and displaying the highest similarity to *V.*
224 *longisporum* CRK15920 protein, decreased with time in the roots of susceptible hop, while its
225 expression in the resistant hop increased. A similar trend of expression was also observed in the
226 shoots of both hop varieties. Gene expression of *Vna7.443* (Figure 4B), which produces a secreted
227 protein (276 aa without cysteines) with the highest similarity to *V. longisporum* CRJ82870 protein,
228 was comparable to *Vna5.694*; it decreased in the roots of susceptible hop and peaked at 12 dpi in the
229 roots of resistant hop. A peak of expression at 12 dpi was also observed in the shoots of susceptible
230 hop, while its expression increased with time in the shoots of resistant hop. Expression of the
231 *Vna8.691* gene (Figure 4C), coding for a small secreted protein (95 aa without cysteines) of unknown

232 function with the highest similarity to *V. longisporum* CRK10461 protein, was highest in the roots of
233 susceptible hop at 6 dpi and then decreased with time of infection. The same trend was also observed
234 in the shoots of susceptible hop. Expression of *Vna8.691* in the roots of resistant plants was constant,
235 and around 200-fold higher than that in ½ CD medium, whereas no expression was detected in the
236 shoots. Interestingly, two lethal pathotype specific genes *VnaUn.279* (Figure 4D), encoding a small
237 secreted protein (92 aa without cysteines) with the highest similarity to *V. dahliae* VdLs.17
238 EGY23483 protein, and *Vna4.761* (Figure 4E), encoding a 186 aa protein with 8 cysteines and the
239 highest similarity to *V. longisporum* CRK16219 protein, had similar gene expression patterns as the
240 virulence-associated *V. nonalfalfae* effector *VnaSSP4.2* (Figure 4F). They were expressed only in the
241 roots and shoots of susceptible hop (with expression levels increasing with time of infection) and
242 barely detected in the resistant plants.

243 **2.3 Identification of novel virulence effector of *V. nonalfalfae***

244 Since all five selected CSEPs were specifically expressed during plant colonization, a reverse
245 genetics approach was used to test their contribution to the virulence of *V. nonalfalfae* in hop.
246 Knockout mutants of *VnaUn.279* displayed only minor wilting symptoms in the susceptible hop
247 (Figure 5), while vegetative growth, fungal morphology and sporulation were not affected. Analysis
248 of the relative area under the disease progress curve (rAUDPC) [63] indicated that four independent
249 *VnaUn.279* knockout mutants displayed statistically significantly lower values of rAUDPC than the
250 wild type fungus (Figure 6A). To understand the progress of disease in time, statistical modelling
251 was undertaken. For illustrative purposes only, disease severity index (DSI) values [42] for
252 $\Delta VnaUn.279$ and wild type fungus were modelled by logistic growth model (Figure 6B). The
253 variability of disease progression in individual hop plants is probably due to the specific nature of
254 *Verticillium* colonization, in which only a few attached hyphae randomly penetrate the root
255 intercellularly [64]. As demonstrated by the inflection point of the $\Delta VnaUn.279$ logistic curve,

256 development of disease symptoms was delayed for 10 days compared to the wild type fungus. Based
257 on the asymptote values, the wilting symptoms were considerably less severe in the mutant than in
258 the wild type fungus. Additionally, fungal biomass assessment with qPCR revealed that 32% of
259 plants were infected with *V. nonalfalfae* $\Delta VnaUn.279$ mutants compared to at least 80% for the wild
260 type fungus. These results indicate that deletion of *VnaUn.279* not only severely reduced *V.*
261 *nonalfalfae* virulence but also significantly affected the fungal infectivity via a yet unknown
262 mechanism.

263 The other tested *V. nonalfalfae* knockout mutants (*Vna5.694*, *Vna7.443* and *Vna8.691* in Figure S3)
264 showed unaffected pathogenicity and no statistical differences in rAUDPC values relative to the wild
265 type. Deletion of *Vna4.761* was not achieved, due to its functional redundancy, since two additional
266 copies with over 95% sequence identity have been found after Blastn search against *V. nonalfalfae*
267 reference genome at two different genomic locations.

268 **3 Discussion**

269 Fungal pathogens have evolved diverse strategies to interact with host plants and secrete various
270 effector molecules to overcome plant defense mechanisms. A recently published genome of xylem-
271 invading Sordariomycete fungus *Verticillium nonalfalfae* [22], a transcriptome study of infected hop
272 [45] and obtained proteomic data of fungal growth on xylem simulating medium [44] have provided
273 an opportunity to screen for proteins that may contribute to fungal virulence in hop. In the current
274 study, a customized bioinformatics pipeline was designed to predict the classical *V. nonalfalfae*
275 secretome and then to refine the secretome based on experimental data to identify candidate secreted
276 effector proteins (CSEPs).

277 The relative secretome size of *V. nonalfalfae* (10.2%) conforms to the nutritional lifestyle of plant
278 pathogens with larger secretome sizes (from 2.9% to 12.1% of the proteomes, with an average of

279 7.4%) and fits in the phylogenetic context with other Pezizomycotina (from 3.7% to 12.1% of the
280 proteomes, with an average of 7.3%) [55]. The majority of proteins (69.5%) in the *V. nonalfalfae*
281 secretome were less than 500 aa residues. In contrast to some plant pathogenic Pezizomycotina,
282 which had remarkable 10-15% enrichment of proteins of up to 100 aa residues [55], only 1.8% of
283 such proteins were found in the *V. nonalfalfae* secretome.

284 The composition of the *V. nonalfalfae* predicted secretome, rich in carbohydrate active enzymes
285 (33%), proteases (11%), lipases/cutinases (4.6%) and oxidoreductases (4%), reflected its nutritional
286 lifestyle as a hemibiotroph and plant vascular pathogen. Hemibiotrophic fungi undergo two phases
287 during the infection process; an initial biotrophic phase, with characteristic expression of small
288 secreted proteins without functional annotation (SSPs), is followed by a necrotrophic stage, which is
289 generally associated with the expression of plant cell wall-degrading enzymes (CWDEs) [8]. Similar
290 to *V. dahliae* and *V. alfalfae* genomes [65], the *V. nonalfalfae* genome encodes more CWDEs per
291 number of secreted proteins than other plant pathogenic fungi [8]. Pectinases, xylanases, cellulases,
292 glucanases, proteases, cutinases and lipases are major classes of CWDEs [66] and play important
293 roles during plant colonization. They may facilitate penetration of the plant roots to reach the xylem
294 vessels, degrade pectin gels and tyloses, formed in response to infection, to spread inside vessels,
295 breakdown insoluble wall polymers to acquire nutrients and contribute to the release of survival
296 structures from dead plant material [65]. In addition to contributing to virulence [67], some CWDEs
297 are recognized as pathogen-associated molecular patterns (PAMPs), which provoke PAMP-triggered
298 immunity [68,69]. On the other hand, *V. dahliae* carbohydrate-binding module family 1 domain-
299 containing proteins may suppress glycoside hydrolase 12 protein-triggered immunity in plants [70].
300 As in the case of *V. dahliae* [65], the *V. nonalfalfae* predicted proteome contains numerous glycoside
301 hydrolases and polysaccharide lyases, most of which are secreted [44]; however, only five glycosyl
302 transferases were determined in the predicted secretome. In contrast to *V. dahliae*, there was almost

303 double the number of carbohydrate esterases in the *V. nonalfalfae* proteome and over half were
304 predicted to be secreted. Other abundant proteins in the *V. nonalfalfae* predicted secretome were acid
305 proteases, subtilisin-like proteases and zinc-dependent metalloproteases. These enzymes probably
306 participate in amino acid acquisition, manipulation of host defenses by degradation of pathogenesis-
307 related proteins, including plant chitinases, and act as virulence factors or as elicitors of defense
308 responses [71,72]. A significant number of lipases, phospholipases and cutinases were determined in
309 the *V. nonalfalfae* predicted secretome and identified in a previous proteomic study [44]. In addition
310 to supplying energy for pathogen growth, lipid hydrolysis is crucial for the production of certain
311 signaling molecules, such as oxylipins, which manipulate the host lipid metabolism and alter plant
312 defense responses [73]. The role of cutinases in pathogenicity is controversial and has been
313 associated with the dissolution of the plant cuticle during penetration, suppression of callose
314 formation, spore attachment and surface signaling [74,75]. Another group of abundant enzymes in *V.*
315 *nonalfalfae* predicted and experimentally determined secretomes were oxidoreductases, in particular
316 FAD-dependent oxidoreductases and GMC oxidoreductases. Oxidoreductases are probably secreted
317 for protection against host-produced reactive oxygen species, such as the generation of H₂O₂, which
318 was detected after infection with *V. dahliae* in cotton roots [76] and in tomato plants [77]. On the
319 other hand, fungal pathogens can actively contribute to the ROS level in host plants [78]. In *V.*
320 *dahliae*, NADPH oxidase complex (Nox), composed of the catalytic subunit *VdNoxB* and tetraspanin
321 *VdPls1*, is responsible for the production of ROS and the formation of penetration peg within the
322 hyphopodium [64]. Moreover, *VdNoxB* regulates the cytoskeletal organization of the *VdSep5*-septin
323 ring that separates the hyphopodium from invasive hyphae and forms a specialized fungus-host
324 penetration interface, where small secreted proteins preferentially accumulate [79].

325 Since small secreted proteins (SSPs) are the least characterized fungal secreted proteins and some
326 have been reported as effectors, we particularly focused on this group of proteins. Various criteria for

327 the determination of SSPs have been reported [12,80,81] but, for comparison purposes, we adopted a
328 definition [55] that considers SSPs proteins with a mature length of ≤ 300 aa residues and proteins
329 with a relative cysteine content of $\geq 5\%$, as well as ≥ 4 cysteine residues, to be small secreted cysteine-
330 rich proteins (SSCP). According to these criteria, the *V. nonalfalfae* predicted secretome contains 310
331 SSPs (32.8% of the predicted secretome) and 46 (4.9% of the secretome) of those belong to SSCPs.
332 These numbers are lower than the average contents of SSPs (49%) and SSCPs (6.7%) determined in
333 fungi of class 2 secretome size (500-1100 secreted proteins) and average contents of SSPs (47%) and
334 SSCPs (7.5%) in the Pezizomycotina group [55]. In a recent study, SSPs with a mature length of \leq
335 300 aa residues were identified in 136 fungal species and compared in terms of taxa and lifestyles
336 [82]. On average, hemibiotrophs and necrotrophs had higher proportions of secreted enzymes, while
337 biotrophs, symbionts and certain hemibiotrophs had the most abundant SSPs. Furthermore, higher
338 numbers of species-specific SSPs (over 100) were associated with biotrophs and symbionts than
339 necrotrophs and saprotrophs (around 30), suggesting that these effectors coevolved with their hosts,
340 while the range was widest for hemibiotrophs. However, no species-specific SSPs have been
341 discovered in *V. nonalfalfae*, while 13 and 19 have been reported in *V. albo-atrum* and *V. dahliae*,
342 respectively [82].

343 Further analysis of the refined *V. nonalfalfae* secretome, comprised of 263 CSEPs, focused in
344 particular on homologs of known effectors from other plant pathogens. Searching for LysM effectors
345 using CAZy module (CBM50) and PFAM domain PF01476 revealed that the *V. nonalfalfae*
346 secretome contains four *in planta* expressed proteins with 2-6 LysM domains, of which Vna2.979 is
347 an ortholog of VDAG_00902 (Table S6), a core LysM effector of *V. dahliae* [27]. The necrosis- and
348 ethylene-inducing-like proteins (NLPs) are a group of widespread conserved effectors that can trigger
349 immune responses and cell death [56]. Similar to other *Verticillium* spp. [19,65], NLP genes are
350 expanded in the *V. nonalfalfae* genome, with seven genes orthologous to *V. dahliae* NLP1-9 and

351 having no ortholog to VdNLP6. All five NLPs with homologs in the PHI database (Table S6) were
352 expressed in hop; the most abundant was Vna7.239 (VdNLP9), in particular in the roots of
353 susceptible hop (Figure S2), suggesting some role in the plant colonization process. Four fungal
354 hydrophobins, characterized by high levels of hydrophobicity and the presence of eight conserved
355 cysteine residues [60], were found in the refined *V. nonalfalfae* secretome and had homologs in the
356 PHI database (Table S6). Although all were expressed in hop, only expression of Vna7.87 was
357 abundant and root-specific. Interestingly, a role in the development of microsclerotia [83] was
358 demonstrated for type II hydrophobin VDH1 from *V. dahliae*, but it was not required for
359 pathogenicity. Further mining of CSEPs for known effectors revealed that *in planta* expressed
360 Vna2.8 and Vna3.54 are homologs of AVR-Pita1, a neutral zinc metalloprotease from *Magnaporthe*
361 *oryzae* [84], and Vna1.1274 was similar to MgSM1, a putative small protein of the Cerato-platanin
362 family [85]. Three *V. nonalfalfae* CSEPs, Vna10.263 and Vna5.719 with high and ubiquitous
363 expression in hop, and Vna9.246 specifically expressed only in susceptible hop, had similarity to
364 *Candida albicans* RBT4, secreted pathogenesis-related proteins [86], while one CSEP was an
365 ortholog of urea amidolyase (DUR1,2), which enables utilization of urea as a sole nitrogen source
366 [87]. Highly expressed secreted protein Vna4.130 had similarity to EMP1, extracellular matrix
367 protein 1 from *Magnaporthe grisea*, which was required for appressorium formation and
368 pathogenicity [88]. Vna7.617, which was putatively secreted and abundantly expressed in susceptible
369 hop, had an ortholog in *Fusarium oxysporum* membrane mucin Msb2, which regulates invasive
370 growth and plant infection upstream of Fmk1 MAPK [89].

371 The remaining *V. nonalfalfae* CSEPs (92%) were hypothetical, predicted and conserved hypothetical
372 proteins with no functional annotation and their temporal gene expression patterns in susceptible and
373 resistant hop were explored to provide some clues to their function (Table S7 and Figure S2). In
374 addition to the already reported effector VnaSSP4.2 [38], several other CSEPs with distinct

375 expression patterns and high levels of expression were found. Among five CSEPs selected for gene
376 functional analysis using a reverse genetics approach, four were predicted as effectors by EffectorP
377 [16] and one had an ortholog in the PHI database, displaying sequence similarity to fungal effector
378 *LaeA*, a regulator of secondary metabolism [90] and morphogenetic fungal virulence factor [91].
379 After comparing the pathogenicity of wild type fungus to CSEPs knockout mutants (Figure 6 and
380 Figure S3), we discovered that the later CSEP, encoded by lethal pathotype specific gene *VnaUn.279*,
381 is a novel virulence factor of *V. nonalfalfae*. $\Delta VnaUn.279$ mutants had diminished infectivity and
382 exhibited severely reduced virulence in hop. Reduced virulence was also reported for a number of
383 *LaeA* deletion mutants from human pathogen *A. fumigatus* [91], plant pathogenic fungi, including *A.*
384 *flavus*, *C. heterostrophus* and several *Fusarium* species [92], as well as entomopathogenic fungus
385 *Beauveria bassiana* [93]. Altogether, these findings justify further investigation of the biological
386 role of *VnaUn.279* in *V. nonalfalfae* pathogenicity.

387 Despite the other selected CSEPs mutants not displaying any virulence associated phenotype, based
388 on their expression profiles, they probably participate in other physiological processes during *V.*
389 *nonalfalfae* infection of hop. Additionally, certain CSEPs may be recognized (and subsequently
390 termed Avr effectors) by plant resistance proteins (R proteins), which are intracellular nucleotide-
391 binding leucine rich repeat (NLR) receptors, via direct (receptor-mediated binding) or indirect
392 (accessory protein-mediated) interactions, resulting in effector triggered immunity (ETI) [94,95]. To
393 support this hypothesis, further testing of CSEPs mutants in the resistant hop cultivar is required and
394 could result in identification of corresponding hop resistance proteins. These may then be exploited
395 in *Verticillium* wilt control by introducing new genetic resistance traits into hop breeding, as already
396 successfully implemented in certain other crops [96].

397 **4 Conclusions**

398 After comprehensively investigating the predicted *V. nonalfalfae* secretome using a diverse
399 bioinformatics approaches and integrating multiple lines of evidence (genomics, transcriptomics and
400 proteomics), several candidate secreted effector proteins were identified among protein-encoding
401 genes. These are of high interest to scientists working on Verticillium wilt and, more generally, on
402 pathogen effectors. Since the majority were non-annotated protein sequences, two strategies were
403 adopted to gather clues about their function. With spatio-temporal gene expression profiling, we
404 identified those candidate effectors that have important roles during *V. nonalfalfae* colonization of
405 hop, while pathogenicity assays with effector knockout mutants revealed the candidates that
406 contribute to fungal pathogenicity in hop. In conclusion, a new virulence effector of *V. nonalfalfae*,
407 encoded by lethal-pathotype specific gene *VnaUn.279*, was identified and will be subject to future
408 functional and structural studies.

409 **5 Material and Methods**

410 **5.1 Microbial strains and cultivation**

411 Sordariomycete fungus *Verticillium nonalfalfae* [1] was obtained from the Slovenian Institute of Hop
412 Research and Brewing fungal collection. Two isolates from infected hop were used, differing in
413 aggressiveness: lethal pathotype (isolate T2) and mild pathotype (isolate Rec) [97]. Fungal mycelium
414 was cultured at room temperature on a half concentration of Czapek Dox broth ($\frac{1}{2}$ CD),
415 supplemented with 1 g/L malt extract, 1 g/L peptone (all from Duchefa, The Netherlands) and 1 g/L
416 yeast extract (Sigma Life Science, USA). For solid media, 15 g/L agar (Duchefa, The Netherlands)
417 was added to $\frac{1}{2}$ CD with supplements. Alternatively, potato dextrose agar (PDA; Biolife Italiana Srl,
418 Italy) or Xylem simulating medium (XSM; [98]) was used.

419 *Escherichia coli* DH5 α , used for amplification of vector constructs, was cultivated in LB medium
420 with 50 mg/L kanamycin (Duchefa, The Netherlands) at 37°C.

421 *Agrobacterium tumefaciens* (LBA4404) transformation was performed in YM medium [99]
422 containing 100 mg/L streptomycin and 50 mg/L kanamycin (both from Duchefa, The Netherlands) at
423 30°C. The co-cultivation of transformed *A. tumefaciens* and *V. nonalfalfae* was carried out on IMAS
424 plates [99] at room temperature.

425 **5.2 Functional annotation of *V. nonalfalfae* gene models and RNA-Seq analysis**

426 Using a customized Genialis Platform (Genialis, Slovenia; [https://www.genialis.com/genialis-](https://www.genialis.com/genialis-platform/)
427 [platform/](https://www.genialis.com/genialis-platform/)), the gene models of the *V. nonalfalfae* reference genome [22] were translated into putative
428 proteins with the ExPASy Translate tool [100] and ORF Finder [101]. The general characteristics of
429 putative proteins (molecular weight, number of amino acids (aa), percentage of cysteines and
430 isoelectric point) were predicted by the ProtParam tool [100]. Functional annotation of the predicted
431 proteins was performed with HMMER searches [102] against CAZy [103,104], Pfam [105], and
432 Superfamily [106], as well as with BLAST searches [107] against NCBI, KOG [108], *MEROPS*
433 [109] and PHI databases [62], followed by Blast2GO [110] and KEGG [111,112] analyses. The
434 overrepresentation of GO terms in the *V. nonalfalfae in-silico* secretome compared to proteome was
435 assessed using a hypergeometric distribution test (HYPGEOM.DIST function in Excel) with a *p*-
436 value < 0.05 and FDR < 0.05.

437 RNA-sequencing of *V. nonalfalfae* mild and lethal pathotypes was performed by IGA Technology
438 Service (Udine, Italy) using Illumina Genome Analyzer II. For this purpose, total RNA, enriched for
439 the polyA mRNA fraction, was isolated in three biological replicates from fungal mycelia of mild
440 and lethal strains grown in xylem-simulating media according to [98]. Illumina raw sequence reads
441 were deposited at NCBI (Bioproject PRJNA283258). RNA-Seq analysis was performed using CLC
442 Genomics Workbench tools (Qiagen, USA). Differentially expressed genes between lethal and mild

443 fungal pathotype were identified as those with fold change $FC \geq 1.5$ or $FC \leq -1.5$ ($p \leq 0.05$; FDR \leq
444 0.05).

445 From our previous RNA-Seq data of compatible and incompatible interactions between hop and *V.*
446 *nonalfalfae* [45], fungal transcripts expressed at a least one time point (6, 12, 18 and 30 dpi) and one
447 hop cultivar (susceptible 'Celeia' or resistant 'Wye Target') were filtered out and data were presented
448 as a matrix of \log_2 CPM (counts per million – number of reads mapped to a gene model per million
449 reads mapped to the library) expression values. These genes were considered as expressed *in planta*.

450 **5.3 Secretome prediction and comparison**

451 The *V. nonalfalfae in silico* secretome was determined using a customized Genialis Platform
452 (Genialis, Slovenia) according to the method described in [113], which reportedly gives 83.4%
453 accuracy for fungal secreted proteins. It combines SignalP4.1 [114], WolfPsort [47] and Phobius [46]
454 for N-terminal signal peptide prediction, TMHMM (<http://www.cbs.dtu.dk/services/TMHMM/>) for
455 eliminating membrane proteins (allowing one transmembrane (TM) domain in the first 60 aa) and
456 PS-Scan [115] for removing proteins with ER targeting sequence (Prosite: PS00014). In addition, we
457 used LOCALIZER [49] to predict effector protein localization to chloroplasts and mitochondria,
458 while proteins with a nuclear localization signal were determined with NucPred (likelihood score
459 >0.80) [116] and PredictNLS [117]. Localization of effector proteins to the apoplast was predicted by
460 ApoplastP [48] based on enrichment in small amino acids and cysteines, as well as depletion in
461 glutamic acid.

462 To compare the composition of the *V. nonalfalfae* secretome to other closely related plant pathogenic
463 *Verticillium* species, protein coding sequences of *Verticillium dahliae* JR2, *Verticillium longisporum*
464 GCA_001268145 and *Verticillium alfalfae* VaMs.102 from the Ensembl Fungi database
465 (<http://fungi.ensembl.org/info/website/ftp/index.html>) were used and secretome predictions,

466 HMMER searches against CAZy database and blastp searches against the *MEROPS* database were
467 performed using the same pipeline as for *V. nonalfalfae*. Two way ANNOVA followed by Tukey's
468 multiple comparisons test (p -value < 0.05) in GraphPad Prism 7.03 (GraphPad Software, Inc., USA)
469 was used to find differences between sets of fungal proteins.

470 **5.4 Refinement of *V. nonalfalfae* secretome and selection of CSEPs**

471 A refinement of total *V. nonalfalfae in silico* secretome (Figure 1) was done to maintain only
472 proteins, transcripts of which were expressed *in planta* according to the RNA-Seq analysis. Proteins
473 with carbohydrate enzymatic activities (CAZy screening) were excluded from further analysis and
474 additional filtering was applied based on the presence of PFAM domains. CSEPs were identified as
475 proteins having known effector-specific domains [9,12,13,16,118], NLS signal or as proteins with no
476 PFAM domains.

477 In the second step, the number of secreted proteins was narrowed down using the following criteria:
478 proteins determined in the lethal pathotype-specific region identified by comparative genomics of
479 mild and lethal *V. nonalfalfae* strains from three geographic regions [22]; proteins differentially
480 expressed in lethal compared to mild *V. nonalfalfae* strains grown in xylem-simulating media as
481 determined by RNA-Seq; *V. nonalfalfae* secreted proteins analyzed by 2D-DIGE and identified by
482 MALDI-TOF/TOF MS [44]; proteins with sequence similarity to experimentally verified
483 pathogenicity, virulence and effector genes in the PHI (Pathogen-host Interaction) database [62] and
484 putative effector proteins predicted by EffectorP software [16].

485 **5.5 Quantitative real time PCR and fungal biomass quantification**

486 Susceptible 'Celeia' and resistant 'Wye Target' hop varieties were inoculated by the root dipping
487 method [119] with *V. nonalfalfae* spores. Total RNA was isolated from the roots and stems of
488 infected plants (6, 12 and 18 dpi) or mock-inoculated plants using a MagMAX total RNA isolation

489 kit (Life Technologies, USA). The quality and quantity of RNA was assessed on an Agilent 2100
490 Bioanalyzer (Agilent Technologies, Germany). Total RNA was transcribed to cDNA with a High
491 Capacity cDNA Reverse Transcription kit (Applied Biosystems, USA). Real-time PCR reactions
492 were performed on 7500 Fast Real Time PCR Systems (Life Technologies, USA) using the FastStart
493 SYBR Green master mix (Roche, Switzerland) and primers (Table S8) designed by Primer Express
494 3.0 software (Thermo Fisher Scientific, USA). For each of the 44 top priority CSEPs, gene
495 expression was analyzed on pooled samples containing the roots of five individual plants, in two
496 technical replicates. The highest expressed CSEPs were also analyzed in five biological and two
497 technical replicates per sample group. The CSEPs' gene expression was calculated by the
498 comparative C_T method [120]. The cDNA from *V. nonalfalfae* mycelium cultivated on ½ CD was
499 used as a reference sample. *V. nonalfalfae* DNA topoisomerase (*VnaUn.148*) and splicing factor 3a2
500 (*Vna8.801*) were selected as the best endogenous control genes according to GeNorm analysis [121]
501 and fungal biomass normalization. For the latter, fungal DNA was extracted from infected hop using
502 CTAB and quantified by qPCR as described in [122]. The expression of control genes was compared
503 to fungal biomass in infected hop using Pearson's correlation coefficient.

504 **5.6 Construction of knockout vectors and preparation of *V. nonalfalfae* knockout mutants**

505 CSEPs knockout mutants were prepared according to Frandsen's protocol [123]. The plasmid vector
506 pRF-HU2 was first linearized with *Nt.BbvCI* and *PacI* (New England BioLabs, USA) and purified
507 with Illustra GFX PCR DNA and Gel Band Purification Kit (GE Healthcare, UK). Homologous gene
508 sequences were then amplified with PCR using a *PfuTurbo Cx* Hotstart DNA polymerase (Agilent
509 Technologies, USA) and the following settings: 95°C for 2 minutes, 30 cycles: 95°C for 30s, 55°C
510 for 30s, 72°C for 1 minute; 75°C for 10 minutes. PCR products were purified with Illustra GFX PCR
511 DNA and a Gel Band Purification Kit (GE Healthcare, UK) and ligated to linearized vector pRF-

512 HU2 with USER enzyme (New England BioLabs, USA). Vector constructs were multiplied in *E. coli*
513 DH5 α cells and isolated with a High Pure Plasmid Isolation Kit (Roche, Life Science, USA).

514 *V. nonalfalfae* knockout mutants were generated with *Agrobacterium tumefaciens* mediated
515 transformation (ATMT) [124] using acetosyringone (Sigma Aldrich, USA). The knockout vector
516 constructs were electroporated with Easyject Prime (EQUIBIO, UK) into electro-competent
517 *Agrobacterium tumefaciens* (LBA4404) cells. Positive colonies with a correct construct orientation
518 were verified by colony PCR. Co-culture of transformed *A. tumefaciens* and *V. nonalfalfae* was
519 carried out on IMAS media as described in [99]. Colonies were transferred on a cellophane
520 membrane (GE Healthcare, UK) to primary and secondary 1/2 CD selection medium with 150 mg/L
521 timentin (Duchefa, The Netherlands) and 75 mg/L hygromycin (Duchefa, The Netherlands).
522 Genomic DNA was isolated according to [125] from the remaining colonies and the knockout was
523 verified with PCR. Transformed *V. nonalfalfae* conidia were stored in 30% glycerol at -80°C until
524 testing.

525 **5.7 Pathogenicity evaluation of *V. nonalfalfae* knockout mutants in hop**

526 Before pathogenicity tests were carried out, fungal growth and conidiation were inspected as
527 described previously [126]. Ten to fifteen plants of the Verticillium wilt susceptible hop cultivar
528 'Celeia' were inoculated at phenological stage BBCH 12 by 10-min root dipping in a conidia
529 suspension of *V. nonalfalfae* knockout mutants as described previously [126]. Conidia of the wild
530 type *V. nonalfalfae* lethal pathotype served as a positive control and sterile distilled water was used
531 as a mock control. Verticillium wilting symptoms were assessed four to five times post inoculation
532 using a disease severity index (DSI) with a 0-5 scale [42], and rAUDPC was calculated according to
533 [63]. After symptom assessment, fungal re-isolation test and qPCR using *V. nonalfalfae* specific
534 primers (Table S8) were performed to confirm infection of hops.

535 **5.8 Statistics**

536 The R package [127] was used for the statistical analysis of the pathogenicity assay of knockout
537 mutants. Due to the different variability of rAUDPC values for the 'isolate' groups, a non-parametric
538 approach was pursued. A Kruskal-Wallis test was used, followed by multiple comparison test with
539 Bonferroni correction. To understand how the time post inoculation with *V. nonalfalfae* affects hop
540 health, a simple logistic growth model [128] was fitted to DSI values for the groups under study.

541 **6 List of Abbreviations**

542 AA - proteins with auxiliary activities

543 ATMT - *Agrobacterium tumefaciens* mediated transformation

544 CBM - proteins with carbohydrate-binding modules

545 CE - carbohydrate esterases

546 CSEPs - candidate secreted effector proteins

547 CWDEs - cell wall-degrading enzymes

548 DSI - disease severity index

549 ETI - effector triggered immunity

550 GH - glycoside hydrolases

551 GT - glycosyltransferases

552 KOG - EuKaryotic Orthologous Groups

553 NLPs - necrosis and ethylene-inducing protein (NEP-1)-like proteins

554 NLR - nucleotide-binding leucine rich repeat

- 555 Nox - NADPH oxidase complex
- 556 PAMPs - pathogen-associated molecular patterns
- 557 PHI - Pathogen-host interaction database
- 558 PL - polysaccharide lyases
- 559 rAUDPC - relative area under the disease progress curve
- 560 ROS – reactive oxygen species
- 561 SSCPs - small secreted cysteine-rich proteins
- 562 SSPs - small secreted proteins
- 563 TM - transmembrane domain
- 564 XSM - xylem simulating medium

565 **7 Declarations**

566 **Ethics approval and consent to participate:** Not applicable.

567 **Consent for publication:** Not applicable.

568 **Availability of data and materials:** All data generated or analyzed during this study are included in
569 this published article and its supplementary information files. *Verticillium nonalfalfae* genomic data
570 are available at NCBI under BioProject [PRJNA283258](https://www.ncbi.nlm.nih.gov/bioproject/PRJNA283258), while transcriptome data of *Verticillium*
571 *nonalfalfae* interaction with hop can be retrieved from NCBI Bioproject [PRJEB14243](https://www.ncbi.nlm.nih.gov/bioproject/PRJEB14243).

572 **Competing Interests:** The authors declare that they have no competing interests.

573 **Funding:** This work was financed by the Slovenian Research Agency grants P4-0077, J4-8220 and
574 342250.

575 **Authors' Contributions:** BJ conceived and coordinated the study and SB participated in its design.
576 JJ performed *Verticillium nonalfalfae* genome assembly and gene model predictions. SR prepared the
577 plant and fungal material and performed hop inoculations. KM and SB performed secretome analysis
578 and RT-qPCR experiments. MF and KM prepared ATMT knockout mutants and performed the
579 pathogenicity assays together with SR. KK performed statistical analysis of data. KM, SB and BJ
580 analyzed and interpreted the data and drafted the manuscript. All authors read and approved the final
581 manuscript.

582 **Acknowledgments:** We express our sincere gratitude to Dr. Vasja Progar and the Genialis team for
583 their help with bioinformatics. We acknowledge advice on data normalization in RT-qPCR
584 experiments by Dr. Nataša Štajner from the University of Ljubljana. We thank Martin Cregeen for
585 English language editing.

586

587 **8 References**

- 588 1. Inderbitzin P, Bostock RM, Davis RM, Usami T, Platt HW, Subbarao K V. Phylogenetics and
589 taxonomy of the fungal vascular wilt pathogen *Verticillium*, with the descriptions of five new species.
590 PLoS One. Public Library of Science; 2011;6:e28341.
- 591 2. Pegg GF, Brady BL. *Verticillium* Wilts. CABI Pub.; 2002.
- 592 3. EFSA PLH Panel (EFSA Panel on Plant Health). Scientific opinion on the pest categorisation of
593 *Verticillium albo-atrum* sensu stricto Reinke and Berthold, *V. alfalfae* Inderb., HW Platt, RM
594 Bostock, RM Davis & KV Subbarao, sp. nov., and *V. nonalfalfae* Inderb., HW Platt, RM Bostock,
595 RM Davis & KV Subbar. EFSA J. 2014.

- 596 4. Inderbitzin P, Subbarao K V. *Verticillium* systematics and evolution: How confusion impedes
597 *Verticillium* wilt management and how to resolve it. *Phytopathology*. 2014;104:564–74.
- 598 5. Klimes A, Dobinson KF, Klosterman SJ, Thomma BPHJ. Genomics spurs rapid advances in our
599 understanding of the basic biology of vascular wilt pathogens in the genus *Verticillium*. *Annu. Rev.*
600 *Phytopathol.* 2014;
- 601 6. Daayf F. *Verticillium* wilts in crop plants: Pathogen invasion and host defence responses. *Can. J.*
602 *Plant Pathol.* 2015;37:8–20.
- 603 7. Kamoun S. The secretome of plant-associated fungi and oomycetes. *The Mycota*. Berlin,
604 Heidelberg: Springer Berlin Heidelberg; 2009. p. 173–80.
- 605 8. Lo Presti L, Lanver D, Schweizer G, Tanaka S, Liang L, Tollot M, et al. Fungal effectors and plant
606 susceptibility. *Annu. Rev. Plant Biol. Annual Reviews*; 2015;66:513–45.
- 607 9. Stergiopoulos I, de Wit PJGM. Fungal effector proteins. *Annu. Rev. Phytopathol.* 2009;47:233–63.
- 608 10. de Jonge R. In silico identification and characterization of effector catalogs. *Methods Mol. Biol.*
609 2012. p. 415–25.
- 610 11. Sperschneider J, Williams AH, Hane JK, Singh KB, Taylor JM. Evaluation of secretion
611 prediction highlights differing approaches needed for oomycete and fungal effectors. *Front. Plant Sci.*
612 *Frontiers Media SA*; 2015;6:1168.
- 613 12. Saunders DGO, Win J, Cano LM, Szabo LJ, Kamoun S, Raffaele S. Using hierarchical clustering
614 of secreted protein families to classify and rank candidate effectors of rust fungi. *PLoS One.*
615 2012;7:e29847.
- 616 13. Guyon K, Balagué C, Roby D, Raffaele S. Secretome analysis reveals effector candidates

- 617 associated with broad host range necrotrophy in the fungal plant pathogen *Sclerotinia sclerotiorum*.
618 BMC Genomics. 2014;15:336.
- 619 14. Sonah H, Deshmukh RK, Bélanger RR. Computational prediction of effector proteins in fungi:
620 Opportunities and challenges. Front. Plant Sci. 2016;7.
- 621 15. Gibriel HAY, Thomma BPHJ, Seidl MF. The age of effectors: Genome-based discovery and
622 applications. Phytopathology. 2016;106:1206–12.
- 623 16. Sperschneider J, Gardiner DM, Dodds PN, Tini F, Covarelli L, Singh KB, et al. EffectorP:
624 predicting fungal effector proteins from secretomes using machine learning. New Phytol.
625 2016;210:743–61.
- 626 17. Klosterman SJ, Subbarao K V, Kang S, Veronese P, Gold SE, Thomma BPHJ, et al. Comparative
627 genomics yields insights into niche adaptation of plant vascular wilt pathogens. PLoS Pathog. Public
628 Library of Science; 2011;7:e1002137.
- 629 18. De Jonge R, Bolton MD, Kombrink A, Van Den Berg GCM, Yadeta KA, Thomma BPHJ.
630 Extensive chromosomal reshuffling drives evolution of virulence in an asexual pathogen. Genome
631 Res. Cold Spring Harbor Laboratory Press; 2013;23:1271–82.
- 632 19. Seidl MF, Faino L, Shi-Kunne X, van den Berg GCM, Bolton MD, Thomma BPHJ. The genome
633 of the saprophytic fungus *Verticillium tricorpus* reveals a complex effector repertoire resembling that
634 of its pathogenic relatives. Mol. Plant-Microbe Interact. The American Phytopathological Society;
635 2015;28:362–73.
- 636 20. Faino L, Seidl MF, Datema E, van den Berg GCM, Janssen A, Wittenberg AHJ, et al. Single-
637 molecule real-time sequencing combined with optical mapping yields completely finished fungal
638 genome. MBio. American Society for Microbiology; 2015;6:e00936-15.

- 639 21. Depotter JRL, Seidl MF, van den Berg GCM, Thomma BPHJ, Wood TA. A distinct and
640 genetically diverse lineage of the hybrid fungal pathogen *Verticillium longisporum* population causes
641 stem striping in British oilseed rape. *Environ. Microbiol.* 2017;19:3997–4009.
- 642 22. Jakše J, Jelen V, Radišek S, de Jonge R, Mandelc S, Majer A, et al. Genome sequence of xylem-
643 invading *Verticillium nonalfalfae* lethal strain. *Genome Announc.* 2018;6:e01458-17.
- 644 23. Sánchez-Vallet A, Saleem-Batcha R, Kombrink A, Hansen G, Valkenburg D-J, Thomma BPHJ,
645 et al. Fungal effector Ecp6 outcompetes host immune receptor for chitin binding through intrachain
646 LysM dimerization. *Elife.* 2013;2:e00790.
- 647 24. Laugé R, Joosten MHAJ, Van den Ackerveken GFJM, Van den Broek HWJ, De Wit PJGM. The
648 In planta-produced extracellular proteins ECP1 and ECP2 of *Cladosporium fulvum* are virulence
649 factors. *Mol. Plant-Microbe Interact. The American Phytopathological Society* ; 1997;10:725–34.
- 650 25. Mentlak TA, Kombrink A, Shinya T, Ryder LS, Otomo I, Saitoh H, et al. Effector-mediated
651 suppression of chitin-triggered immunity by *Magnaporthe oryzae* is necessary for rice blast disease.
652 *Plant Cell.* 2012;24:322–35.
- 653 26. Takahara H, Hacquard S, Kombrink A, Hughes HB, Halder V, Robin GP, et al. *Colletotrichum*
654 *higginsianum* extracellular LysM proteins play dual roles in appressorial function and suppression of
655 chitin-triggered plant immunity. *New Phytol.* 2016;211:1323–37.
- 656 27. Kombrink A, Rovenich H, Shi-Kunne X, Rojas-Padilla E, van den Berg GCM, Domazakis E, et
657 al. *Verticillium dahliae* LysM effectors differentially contribute to virulence on plant hosts. *Mol.*
658 *Plant Pathol.* 2017;18:596–608.
- 659 28. de Jonge R, Peter van Esse H, Kombrink A, Shinya T, Desaki Y, Bours R, et al. Conserved
660 fungal LysM effector Ecp6 prevents chitin-triggered immunity in plants. *Science* (80-.).

- 661 2010;329:953–5.
- 662 29. Zhou B-J, Jia P-S, Gao F, Guo H-S. Molecular characterization and functional analysis of a
663 Necrosis- and ethylene-Inducing, protein-encoding gene family from *Verticillium dahliae*. Mol.
664 Plant-Microbe Interact. The American Phytopathological Society; 2012;25:964–75.
- 665 30. Santhanam P, van Esse HP, Albert I, Faino L, Nürnberger T, Thomma BPHJ. Evidence for
666 functional diversification within a fungal NEP1-like protein family. Mol. Plant. Microbe. Interact.
667 2013;26:278–86.
- 668 31. de Jonge R, van Esse HP, Maruthachalam K, Bolton MD, Santhanam P, Saber MK, et al. Tomato
669 immune receptor Ve1 recognizes effector of multiple fungal pathogens uncovered by genome and
670 RNA sequencing. Proc. Natl. Acad. Sci. National Acad Sciences; 2012;109:5110–5.
- 671 32. Fradin EF, Abd-El-Haliem A, Masini L, van den Berg GCM, Joosten MHAJ, Thomma BPHJ.
672 Interfamily transfer of tomato Ve1 mediates *Verticillium* resistance in *Arabidopsis*. Plant Physiol.
673 2011;156:2255–65.
- 674 33. Fradin EF, Zhang Z, Rovenich H, Song Y, Liebrand TWH, Masini L, et al. Functional analysis of
675 the tomato immune receptor Ve1 through domain swaps with its non-functional homolog Ve2. PLoS
676 One. 2014;9:e88208.
- 677 34. Liu W, Zeng H, Liu Z, Yang X, Guo L, Qiu D. Mutational analysis of the *Verticillium dahliae*
678 protein elicitor PevD1 identifies distinctive regions responsible for hypersensitive response and
679 systemic acquired resistance in tobacco. Microbiol. Res. Elsevier GmbH.; 2014;169:476–82.
- 680 35. Wang B, Yang X, Zeng H, Liu H, Zhou T, Tan B, et al. The purification and characterization of a
681 novel hypersensitive-like response-inducing elicitor from *Verticillium dahliae* that induces resistance
682 responses in tobacco. Appl. Microbiol. Biotechnol. 2012;93:191–201.

- 683 36. Bu B, Qiu D, Zeng H, Guo L, Yuan J, Yang X. A fungal protein elicitor PevD1 induces
684 *Verticillium* wilt resistance in cotton. *Plant Cell Rep.* 2014;33:461–70.
- 685 37. Zhang L, Ni H, Du X, Wang S, Ma XW, Nürnberger T, et al. The *Verticillium*-specific protein
686 VdSCP7 localizes to the plant nucleus and modulates immunity to fungal infections. *New Phytol.*
687 2017;215:368–81.
- 688 38. Flajšman M, Mandelc S, Radišek S, Štajner N, Jakše J, Košmelj K, et al. Identification of novel
689 virulence-associated proteins secreted to xylem by *Verticillium nonalfalfae* during colonization of
690 hop plants. *Mol. Plant. Microbe. Interact.* 2016;29:362–73.
- 691 39. Keyworth WG. *Verticillium* wilt of the hop (*Humulus lupulus*). *Ann. Appl. Biol. Blackwell*
692 *Publishing Ltd;* 1942;29:346–57.
- 693 40. Sewell GWF, Wilson JF. The nature and distribution of *Verticillium albo-atrum* strains highly
694 pathogenic to the hop. *Plant Pathol. Wiley Online Library;* 1984;33:39–51.
- 695 41. Talboys PW. Resistance to vascular wilt fungi. *Proc. R. Soc. London. Ser. B. Biol. Sci. The*
696 *Royal Society;* 1972;181:319–32.
- 697 42. Radišek S, Jakše J, Simončič A, Javornik B. Characterization of *Verticillium albo-atrum* field
698 isolates using pathogenicity data and AFLP analysis. *Plant Dis.* 2003;87:633–8.
- 699 43. Radišek S, Jakše J, Javornik B. Genetic variability and virulence among *Verticillium albo-atrum*
700 isolates from hop. *Eur. J. plant Pathol. Springer;* 2006;116:301–14.
- 701 44. Mandelc S, Javornik B. The secretome of vascular wilt pathogen *Verticillium albo-atrum* in
702 simulated xylem fluid. *Proteomics.* 2015;15:787–97.
- 703 45. Progar V, Jakše J, Štajner N, Radišek S, Javornik B, Berne S. Comparative transcriptional

- 704 analysis of hop responses to infection with *Verticillium nonalfalfae*. Plant Cell Rep. Springer Berlin
705 Heidelberg; 2017;36:1599–613.
- 706 46. Käll L, Krogh A, Sonnhammer ELL. A combined transmembrane topology and signal peptide
707 prediction method. J. Mol. Biol. 2004;338:1027–36.
- 708 47. Horton P, Park K-J, Obayashi T, Fujita N, Harada H, Adams-Collier CJ, et al. WoLF PSORT:
709 protein localization predictor. Nucleic Acids Res. 2007;35:W585-7.
- 710 48. Sperschneider J, Dodds PN, Singh KB, Taylor JM. ApoplastP: prediction of effectors and plant
711 proteins in the apoplast using machine learning. doi.org. Cold Spring Harbor Laboratory;
712 2017;182428.
- 713 49. Sperschneider J, Catanzariti A-M, DeBoer K, Petre B, Gardiner DM, Singh KB, et al.
714 LOCALIZER: subcellular localization prediction of both plant and effector proteins in the plant cell.
715 Sci. Rep. Nature Publishing Group; 2017;7:44598.
- 716 50. Wilson D, Pethica R, Zhou Y, Talbot C, Vogel C, Madera M, et al. SUPERFAMILY--
717 sophisticated comparative genomics, data mining, visualization and phylogeny. Nucleic Acids Res.
718 Oxford University Press; 2009;37:D380-6.
- 719 51. Macdonald SS, Blaukopf M, Withers SG. *N*-acetylglucosaminidases from CAZy family GH3 are
720 really glycoside phosphorylases, thereby explaining their use of histidine as an acid/base catalyst in
721 place of glutamic acid. J. Biol. Chem. 2015;290:4887–95.
- 722 52. Aspeborg H, Coutinho PM, Wang Y, Brumer H, Henrissat B. Evolution, substrate specificity and
723 subfamily classification of glycoside hydrolase family 5 (GH5). BMC Evol. Biol. 2012;12:186.
- 724 53. Mewis K, Lenfant N, Lombard V, Henrissat B. Dividing the large glycoside hydrolase family 43

- 725 into subfamilies: a motivation for detailed enzyme characterization. Nojiri H, editor. Appl. Environ.
726 Microbiol. 2016;82:1686–92.
- 727 54. Akcapinar GB, Kappel L, Sezerman OU, Seidl-Seiboth V. Molecular diversity of LysM
728 carbohydrate-binding motifs in fungi. Curr. Genet. 2015;61:103–13.
- 729 55. Krijger J-J, Thon MR, Deising HB, Wirsel SG. Compositions of fungal secretomes indicate a
730 greater impact of phylogenetic history than lifestyle adaptation. BMC Genomics. 2014;15:722.
- 731 56. Gijzen M, Nürnberger T. Nep1-like proteins from plant pathogens: recruitment and
732 diversification of the NPP1 domain across taxa. Phytochemistry. 2006;67:1800–7.
- 733 57. Stergiopoulos I, Kourmpetis YAI, Slot JC, Bakker FT, De Wit PJGM, Rokas A. In silico
734 characterization and molecular evolutionary analysis of a novel superfamily of fungal effector
735 proteins. Mol. Biol. Evol. 2012;29:3371–84.
- 736 58. Baccelli I. Cerato-platanin family proteins: one function for multiple biological roles? Front.
737 Plant Sci. Frontiers Media SA; 2014;5:769.
- 738 59. Koharudin LMI, Viscomi AR, Montanini B, Kershaw MJ, Talbot NJ, Ottonello S, et al.
739 Structure-function analysis of a CVNH-LysM lectin expressed during plant infection by the rice blast
740 fungus *Magnaporthe oryzae*. Structure. NIH Public Access; 2011;19:662–74.
- 741 60. Bayry J, Aïmanianda V, Guijarro JI, Sunde M, Latgé J-P. Hydrophobins - unique fungal proteins.
742 PLoS Pathog. Public Library of Science; 2012;8:e1002700.
- 743 61. Kulkarni RD, Kelkar HS, Dean RA. An eight-cysteine-containing CFEM domain unique to a
744 group of fungal membrane proteins. Trends Biochem. Sci. 2003;28:118–21.
- 745 62. Urban M, Pant R, Raghunath A, Irvine AG, Pedro H, Hammond-Kosack KE. The Pathogen-Host

- 746 Interactions database (PHI-base): additions and future developments. *Nucleic Acids Res.*
747 2015;43:D645–55.
- 748 63. Simko I, Piepho H-P. The area under the disease progress stairs: calculation, advantage, and
749 application. *Phytopathology.* 2012;102:381–9.
- 750 64. Zhao Y-L, Zhou T-T, Guo H-S. Hyphopodium-specific VdNoxB/VdPls1-dependent ROS-Ca²⁺
751 signaling is required for plant infection by *Verticillium dahliae*. Wilson RA, editor. *PLOS Pathog.*
752 2016;12:e1005793.
- 753 65. Klosterman SJ, Subbarao K V, Kang S, Veronese P, Gold SE, Thomma BPHJ, et al. Comparative
754 genomics yields insights into niche adaptation of plant vascular wilt pathogens. Dangl JL, editor.
755 *PLoS Pathog.* Public Library of Science; 2011;7:e1002137.
- 756 66. Di Pietro A, Roncero MIG, Roldán MCR. From tools of survival to weapons of destruction: The
757 role of cell wall-degrading enzymes in plant infection. In: Deising HB, editor. *Plant Relationships.*
758 Berlin, Heidelberg: Springer Berlin Heidelberg; 2009. p. 181–200.
- 759 67. Kubicek CP, Starr TL, Glass NL. Plant cell wall-degrading enzymes and their secretion in plant-
760 pathogenic fungi. *Annu. Rev. Phytopathol.* 2014;52:427–51.
- 761 68. Ma Z, Song T, Zhu L, Ye W, Wang Y, Shao Y, et al. A *Phytophthora sojae* glycoside hydrolase
762 12 protein is a major virulence factor during soybean infection and is recognized as a PAMP. *Plant*
763 *Cell.* 2015;27:2057–72.
- 764 69. Zhang L, Kars I, Essenstam B, Liebrand TWH, Wagemakers L, Elberse J, et al. Fungal
765 Endopolygalacturonases are recognized as microbe-associated molecular patterns by the *Arabidopsis*
766 receptor-like protein RESPONSIVENESS TO BOTRYTIS POLYGALACTURONASES1. *Plant*
767 *Physiol.* American Society of Plant Biologists; 2014;164:352–64.

- 768 70. Gui Y-J, Chen J-Y, Zhang D-D, Li N-Y, Li T-G, Zhang W-Q, et al. *Verticillium dahliae*
769 manipulates plant immunity by glycoside hydrolase 12 proteins in conjunction with carbohydrate-
770 binding module 1. *Environ. Microbiol.* 2017;19:1914–32.
- 771 71. Jashni MK, Mehrabi R, Collemare J, Mesarich CH, de Wit PJGM. The battle in the apoplast:
772 further insights into the roles of proteases and their inhibitors in plant–pathogen interactions. *Front.*
773 *Plant Sci.* 2015;6:584.
- 774 72. Chandrasekaran M, Thangavelu B, Chun SC, Sathiyabama M. Proteases from phytopathogenic
775 fungi and their importance in phytopathogenicity. *J. Gen. Plant Pathol.* 2016;82:233–9.
- 776 73. Zeilinger S, Gupta VK, Dahms TES, Silva RN, Singh HB, Upadhyay RS, et al. Friends or foes?
777 Emerging insights from fungal interactions with plants. *FEMS Microbiol. Rev.* 2016;40.
- 778 74. Serrano M, Coluccia F, Torres M, L’Haridon F, Métraux J-P. The cuticle and plant defense to
779 pathogens. *Front. Plant Sci. Frontiers*; 2014;5:274.
- 780 75. Blümke A, Falter C, Herrfurth C, Sode B, Bode R, Schäfer W, et al. Secreted fungal effector
781 lipase releases free fatty acids to inhibit innate immunity-related callose formation during wheat head
782 infection. *Plant Physiol. American Society of Plant Biologists*; 2014;165:346–58.
- 783 76. Xie C, Wang C, Wang X, Yang X. Proteomics-based analysis reveals that *Verticillium dahliae*
784 toxin induces cell death by modifying the synthesis of host proteins. *J. Gen. Plant Pathol. Springer*
785 *Japan*; 2013;79:335–45.
- 786 77. Gayoso C, Pomar F, Novo-Uzal E, Merino F, de Ilárduya OM. The Ve-mediated resistance
787 response of the tomato to *Verticillium dahliae* involves H₂O₂, peroxidase and lignins and drives PAL
788 gene expression. *BMC Plant Biol.* 2010;10:232.

- 789 78. Heller J, Tudzynski P. Reactive oxygen species in phytopathogenic fungi: Signaling,
790 development, and disease. *Annu. Rev. Phytopathol.* 2011;49:369–90.
- 791 79. Zhou T-T, Zhao Y-L, Guo H-S, Kikuchi S, Arioka M. Secretory proteins are delivered to the
792 septin-organized penetration interface during root infection by *Verticillium dahliae*. Talbot NJ,
793 editor. *PLOS Pathog.* Public Library of Science; 2017;13:e1006275.
- 794 80. Ma L-J, van der Does HC, Borkovich KA, Coleman JJ, Daboussi M-J, Di Pietro A, et al.
795 Comparative genomics reveals mobile pathogenicity chromosomes in *Fusarium*. *Nature*.
796 2010;464:367–73.
- 797 81. Gan P, Ikeda K, Irieda H, Narusaka M, O’Connell RJ, Narusaka Y, et al. Comparative genomic
798 and transcriptomic analyses reveal the hemibiotrophic stage shift of *Colletotrichum* fungi. *New*
799 *Phytol.* 2013;197:1236–49.
- 800 82. Kim K-T, Jeon J, Choi J, Cheong K, Song H, Choi G, et al. Kingdom-wide analysis of fungal
801 small secreted proteins (SSPs) reveals their potential role in host association. *Front. Plant Sci.*
802 *Frontiers Media SA*; 2016;7:186.
- 803 83. Klimes A, Dobinson KF. A hydrophobin gene, VDH1, is involved in microsclerotial
804 development and spore viability in the plant pathogen *Verticillium dahliae*. *Fungal Genet. Biol.*
805 2006;43:283–94.
- 806 84. Jia Y, Zhou E, Lee S, Bianco T. Coevolutionary dynamics of rice blast resistance gene *Pi-ta* and
807 *Magnaporthe oryzae* avirulence gene *AVR-Pita 1*. *Phytopathology*. *Phytopathology*; 2016;106:676–
808 83.
- 809 85. Yang Y, Zhang H, Li G, Li W, Wang X, Song F. Ectopic expression of MgSM1, a Cerato-
810 platanin family protein from *Magnaporthe grisea*, confers broad-spectrum disease resistance in

- 811 *Arabidopsis*. Plant Biotechnol. J. 2009;7:763–77.
- 812 86. Röhm M, Lindemann E, Hiller E, Ermert D, Lemuth K, Trkulja D, et al. A family of secreted
813 pathogenesis-related proteins in *Candida albicans*. Mol. Microbiol. 2013;87:132–51.
- 814 87. Navarathna DHMLP, Lionakis MS, Lizak MJ, Munasinghe J, Nickerson KW, Roberts DD. Urea
815 amidolyase (DUR1,2) contributes to virulence and kidney pathogenesis of *Candida albicans*.
816 Chauhan N, editor. PLoS One. 2012;7:e48475.
- 817 88. Ahn N, Kim S, Choi W, Im K-H, Lee Y-H. Extracellular matrix protein gene, EMP1, is required
818 for appressorium formation and pathogenicity of the rice blast fungus, *Magnaporthe grisea*. Mol.
819 Cells. 2004;17:166–73.
- 820 89. Perez-Nadales E, Di Pietro A. The membrane mucin Msb2 regulates invasive growth and plant
821 infection in *Fusarium oxysporum*. Plant Cell. 2011;23:1171–85.
- 822 90. Bok JW, Keller NP. LaeA, a regulator of secondary metabolism in *Aspergillus* spp. Eukaryot.
823 Cell. 2004;3:527–35.
- 824 91. Bok JW, Balajee SA, Marr KA, Andes D, Nielsen KF, Frisvad JC, et al. LaeA, a regulator of
825 morphogenetic fungal virulence factors. Eukaryot. Cell. American Society for Microbiology (ASM);
826 2005;4:1574–82.
- 827 92. Sarikaya-Bayram Ñ, Palmer JM, Keller N, Braus GH, Bayram Ñ. One Juliet and four Romeos:
828 VeA and its methyltransferases. Front. Microbiol. 2015;6:1.
- 829 93. Qin Y, Ortiz-Urquiza A, Keyhani NO. A putative methyltransferase, mtrA, contributes to
830 development, spore viability, protein secretion and virulence in the entomopathogenic fungus
831 *Beauveria bassiana*. Microbiology. 2014;160:2526–37.

- 832 94. Dodds PN, Rathjen JP. Plant immunity: towards an integrated view of plant-pathogen
833 interactions. *Nat. Rev. Genet.* 2010;11:539–48.
- 834 95. Cui H, Tsuda K, Parker JE. Effector-triggered immunity: from pathogen perception to robust
835 defense. *Annu. Rev. Plant Biol.* 2015;66:487–511.
- 836 96. Vleeshouwers VGAA, Oliver RP. Effectors as tools in disease resistance breeding against
837 biotrophic, hemibiotrophic, and necrotrophic plant pathogens. *Mol. Plant-Microbe Interact.* 27:196–
838 206.
- 839 97. Radišek S, Jakše J, Javornik B. Development of pathotype-specific SCAR markers for detection
840 of *Verticillium albo-atrum* isolates from hop. *Plant Dis.* 2004;88:1115–22.
- 841 98. Neumann MJ, Dobinson KF. Sequence tag analysis of gene expression during pathogenic growth
842 and microsclerotia development in the vascular wilt pathogen *Verticillium dahliae*. *Fungal Genet.*
843 *Biol.* 2003;38:54–62.
- 844 99. Frandsen RJN, Frandsen M, Giese H. *Plant Fungal Pathogens.* 2012;835:17–45.
- 845 100. Gasteiger E, Gattiker A, Hoogland C, Ivanyi I, Appel DR, Bairoch A. ExPASy: the proteomics
846 server for in-depth protein knowledge and analysis. *Nucleic Acids Res.* 2003;31:3784–8.
- 847 101. Wheeler DL, Church DM, Federhen S, Lash AE, Madden TL, Pontius JU, et al. Database
848 resources of the National Center for Biotechnology. *Nucleic Acids Res.* 2003;31:28–33.
- 849 102. Finn RD, Clements J, Eddy SR. HMMER web server: interactive sequence similarity searching.
850 *Nucleic Acids Res.* 2011;39:W29-37.
- 851 103. Cantarel BL, Coutinho PM, Rancurel C, Bernard T, Lombard V, Henrissat B. The
852 Carbohydrate-Active EnZymes database (CAZy): an expert resource for glycogenomics. *Nucleic*

- 853 Acids Res. 2009;37:D233-8.
- 854 104. Lombard V, Golaconda Ramulu H, Drula E, Coutinho PM, Henrissat B. The carbohydrate-
855 active enzymes database (CAZy) in 2013. Nucleic Acids Res. 2014;42:D490-5.
- 856 105. Finn RD, Bateman A, Clements J, Coggill P, Eberhardt RY, Eddy SR, et al. Pfam: The protein
857 families database. Nucleic Acids Res. 2014;42:222–30.
- 858 106. Gough J, Karplus K, Hughey R, Chothia C. Assignment of homology to genome sequences
859 using a library of hidden Markov models that represent all proteins of known structure. J. Mol. Biol.
860 2001;313:903–19.
- 861 107. Altschul SF, Gish W, Miller W, Myers EW, Lipman DJ. Basic local alignment search tool. J.
862 Mol. Biol. 1990;215:403–10.
- 863 108. Tatusov RL, Fedorova ND, Jackson JD, Jacobs AR, Kiryutin B, Koonin E V, et al. The COG
864 database: an updated version includes eukaryotes. BMC Bioinformatics. 2003;4:41.
- 865 109. Rawlings ND, Barrett AJ, Bateman A. MEROPS: the database of proteolytic enzymes, their
866 substrates and inhibitors. Nucleic Acids Res. 2012;40:D343–50.
- 867 110. Conesa A, Götz S, García-Gómez JM, Terol J, Talón M, Robles M. Blast2GO: a universal tool
868 for annotation, visualization and analysis in functional genomics research. Bioinformatics.
869 2005;21:3674–6.
- 870 111. Kanehisa M, Goto S. KEGG: kyoto encyclopedia of genes and genomes. Nucleic Acids Res.
871 2000;28:27–30.
- 872 112. Kanehisa M, Goto S, Sato Y, Kawashima M, Furumichi M, Tanabe M. Data, information,
873 knowledge and principle: back to metabolism in KEGG. Nucleic Acids Res. 2014;42:D199-205.

- 874 113. Min XJ. Evaluation of computational methods for secreted protein prediction in different
875 eukaryotes. 2010;3:143–7.
- 876 114. Petersen TN, Brunak S, von Heijne G, Nielsen H. SignalP 4.0: discriminating signal peptides
877 from transmembrane regions. Nat. Methods. Nature Publishing Group, a division of Macmillan
878 Publishers Limited. All Rights Reserved.; 2011;8:785–6.
- 879 115. de Castro E, Sigrist CJA, Gattiker A, Bulliard V, Langendijk-Genevaux PS, Gasteiger E, et al.
880 ScanProsite: detection of PROSITE signature matches and ProRule-associated functional and
881 structural residues in proteins. Nucleic Acids Res. 2006;34:W362–5.
- 882 116. Brameier M, Krings A, MacCallum RM. NucPred--predicting nuclear localization of proteins.
883 Bioinformatics. 2007;23:1159–60.
- 884 117. Cokol M, Nair R, Rost B. Finding nuclear localization signals. EMBO Rep. 2000;1:411–5.
- 885 118. Heard S, Brown NA, Hammond-Kosack K. An interspecies comparative analysis of the
886 predicted secretomes of the necrotrophic plant pathogens *Sclerotinia sclerotiorum* and *Botrytis*
887 *cinerea*. PLoS One. 2015;10:e0130534.
- 888 119. Mandelc S, Timperman I, Radišek S, Devreese B, Samyn B, Javornik B. Comparative
889 proteomic profiling in compatible and incompatible interactions between hop roots and *Verticillium*
890 *albo-atrum*. Plant Physiol Biochem. 2013;68:23–31.
- 891 120. Schmittgen TD, Livak KJ. Analyzing real-time PCR data by the comparative C(T) method. Nat.
892 Protoc. 2008;3:1101–8.
- 893 121. Schlotter YM, Veenhof EZ, Brinkhof B, Rutten VPMG, Spee B, Willemsse T, et al. A GeNorm
894 algorithm-based selection of reference genes for quantitative real-time PCR in skin biopsies of

- 895 healthy dogs and dogs with atopic dermatitis. *Vet. Immunol. Immunopathol.* 2009;129:115–8.
- 896 122. Cregeen S, Radišek S, Mandelc S, Turk B, Štajner N, Jakše J, et al. Different gene expressions
897 of resistant and susceptible hop cultivars in response to infection with a highly aggressive strain of
898 *Verticillium albo-atrum*. *Plant Mol. Biol. Rep.* 2015;33:689–704.
- 899 123. Frandsen RJN, Andersson J a, Kristensen MB, Giese H. Efficient four fragment cloning for the
900 construction of vectors for targeted gene replacement in filamentous fungi. *BMC Mol. Biol.*
901 2008;9:70.
- 902 124. Knight CJ, Bailey AM, Foster GD. *Agrobacterium*-mediated transformation of the plant
903 pathogenic fungus *Verticillium albo-atrum*. *J. Plant Pathol.* 2009;91:745–50.
- 904 125. Möller EM, Bahnweg G, Sandermann H, Geiger HH. A simple and efficient protocol for
905 isolation of high molecular weight DNA from filamentous fungi, fruit bodies, and infected plant
906 tissues. *Nucleic Acids Res.* 1992;20:6115–6.
- 907 126. Flajšman M, Radišek S, Javornik B. Pathogenicity assay of *Verticillium nonalfalfae* on hop
908 plants. *Bio-protocol.* 2017;7:e2171.
- 909 127. R Core Team. R: A language and environment for statistical computing. Vienna, Austria; 2016.
- 910 128. Pinheiro JC, Bates DM. Mixed-effects models in S and S-PLUS. Springer; 2000.
- 911 129. Robinson MD, Oshlack A. A scaling normalization method for differential expression analysis
912 of RNA-seq data. *Genome Biol. BioMed Central*; 2010;11:R25.

913 **9 Figure captions**

914 **Figure 1.** Bioinformatics pipeline for secretome prediction, identification and characterization of *V.*
915 *nonalfalfae* candidate secreted effector proteins (CSEPs). *V. nonalfalfae* predicted proteome was first
916 filtered based on signal peptide, transmembrane domains and subcellular localization to determine
917 classically secreted proteins. This total predicted secretome was then refined to proteins expressed *in*
918 *planta* and carbohydrate active enzymes were removed so that only proteins with effector-specific
919 PFAM domains, NLS signal or no PFAM domains were retained in the final dataset of 263 CSEPs.
920 These were narrowed down to 44 top-priority candidates based on the results of RNA-Seq and 2D-
921 DIGE analyses, sequence similarity searching to known effectors in the PHI database and EffectorP
922 prediction.

923 **Figure 2.** Classification of the *V. nonalfalfae* predicted secreted proteins into functional groups based
924 on the Superfamily annotation scheme. Groups were classified after [50].

925 **Figure 3.** Relative abundance of carbohydrate-active enzymes (CAZymes), peptidases and small
926 secreted proteins within secretomes of plant pathogenic *Verticillium* species. (A) Comparison of
927 CAZymes from different classes is presented in percentages of predicted fungal secretome. CE,
928 carbohydrate esterase; GH, glycoside hydrolase; GT, glycosyl transferase; PL, polysaccharide lyase;
929 CBM, proteins with carbohydrate-binding modules; AA, proteins with auxiliary activities. (B)
930 Comparison of various classes of peptidases depicted as percentage of predicted fungal secretome.
931 (C) Relative abundance of small secreted proteins and small secreted cysteine rich proteins in
932 predicted fungal secretomes. SSPs, small secreted proteins with less than 300 aa; SSCPs, small
933 secreted proteins with more than 5% cysteine content and at least 4 Cys residues [55]; *Vna*, *V.*
934 *nonalfalfae*; *Va*, *V. alfalfae*; *Vd*, *V. dahliae*; *Vl*, *V. longisporum*.

935 **Figure 4.** Gene expression profiles of selected *V. nonalfalfae* CSEPs in the roots and shoots of
936 infected hop. FC, fold change in gene expression was determined by quantitative real-time PCR
937 using topoisomerase and splicing factor 3a2 as endogenous controls and fungal samples grown on ½

938 CD medium as a reference. Means \pm SEM (n=5) are presented. Statistical significance was
939 determined with the t-test using the Holm-Sidak approach, with $\alpha = 5\%$. 'Celeia', *Verticillium* wilt
940 susceptible hop; 'Wye Target', *Verticillium* wilt resistant hop; dpi, days post inoculation

941 **Figure 5.** Pathogenicity testing in susceptible hop 'Celeia'. Pictures were taken 31 days post
942 inoculation of hop roots with *V. nonalfalfae* conidia suspension. (A) mock-inoculated plants; (B)
943 plants inoculated with wild type *V. nonalfalfae* T2 strain; (C and D), plants inoculated with *V.*
944 *nonalfalfae* $\Delta VnaUn.279$ mutant strains (two replicates).

945 **Figure 6.** *V. nonalfalfae* knockout mutant $\Delta VnaUn.279$ showed severely reduced virulence. (A)
946 Relative area under the disease progress curve (rAUDPC) is presented for knockout mutant
947 $\Delta VnaUn.279$ and for wild type (wt) *V. nonalfalfae*. Darker dots depict double values. A Kruskal-
948 Wallis test followed by multiple comparison test resulted in two groups: *a* for $\Delta VnaUn.279$ and *b* for
949 wild type. (B) Disease severity index (DSI) values were fitted by a simple logistic growth model for
950 mutant $\Delta VnaUn.279$ and for wild type *V. nonalfalfae* hop isolates. The upper horizontal line is the
951 asymptote (black for $\Delta VnaUn.279$, red for wt); the vertical lines show the inflection points (black for
952 $\Delta VnaUn.279$, red for wt) at which the predicted DSI is one half of the asymptote.

953 **10 Additional files**

954 Additional file 1. An Excel file containing 8 tables, each in a separate worksheet.

955 Table S1. *V. nonalfalfae* secretome predicted using Genialis bioinformatics platform. Gene IDs
956 marked in bold represent 263 proteins in the CSEPs catalogue. 2D-DIGE, proteins secreted by mild
957 and lethal strains of *V. nonalfalfae* growing in xylem simulating medium (XSM) were analysed by
958 2D-DIGE and identified by MALDI-TOF/TOF MS [44]; RNA-Seq, differential fungal gene
959 expression (fold change, $FC \geq 1.5$ or $FC \leq -1.5$) of *V. nonalfalfae* lethal versus mild fungal pathotype
960 growing in XSM; LOCALIZER, a tool for subcellular localization prediction of both plant and

961 effector proteins in the plant cell [49]; ApoplastP, a tool for prediction of effectors and plant proteins
962 in the apoplast using machine learning [48].

963 Table S2. KOG functional annotation of *V. nonalfalfae* predicted secretome. KOG, a database of
964 euKaryotic Orthologous Groups from NCBI that allows identification of ortholog and paralog
965 proteins [108].

966 Table S3. *MEROPS* classification of predicted *V. nonalfalfae* secretome. *MEROPS*, a database of
967 peptidases and the proteins that inhibit them [109].

968 Table S4. Assignment of KEGG accessions to the predicted *V. nonalfalfae* secreted proteins. KEGG,
969 the Kyoto Encyclopedia of Genes and Genomes is a database resource for understanding high-level
970 functions and utilities of the biological systems [111].

971 Table S5. List of PFAM domains identified in the predicted *V. nonalfalfae* secretome. PFAM, a
972 collection of protein families, represented by multiple sequence alignments and hidden Markov
973 models (HMMs) [105].

974 Table S6. List of *V. nonalfalfae* CSEPs, including EffectorP prediction and similarity to effectors in
975 the PHI database. EffectorP, a machine learning prediction program for fungal effectors [16]; PHI,
976 Pathogen-Host Interaction database, which contains expertly curated molecular and biological
977 information on genes proven to affect the outcome of pathogen-host interactions [62].

978 Table S7. Bulk expression of best ranked *V. nonalfalfae* candidate effector genes in hop roots. Gene
979 expression was calculated by the comparative C_T method [120]. Hop plants were inoculated by the
980 root dipping method with *V. nonalfalfae* conidia and sampled at 6, 12 and 18 days post inoculation.
981 Analyzed samples contained the roots of five individual plants from either susceptible hop variety
982 'Celeia' (CE) or resistant 'Wye Target' (WT). cDNA from *V. nonalfalfae* mycelium cultivated on ½
983 Czapek Dox (CD) medium was used as a reference sample. *V. nonalfalfae* DNA topoisomerase
984 (*VnaUn.148*) and splicing factor 3a2 (*Vna8.801*) were used as endogenous control genes. Numbers

985 represent log₂ fold changes in the expression of genes in infected plants at indicated time points
986 compared to gene expression in ½ CD medium. *na*, not available

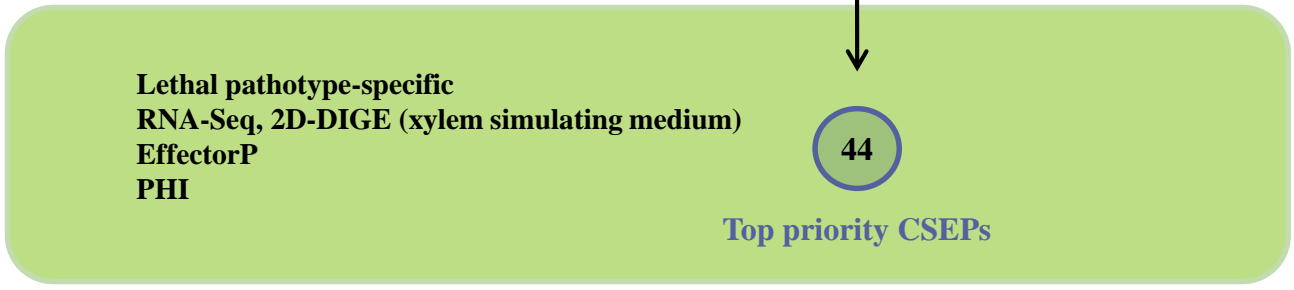
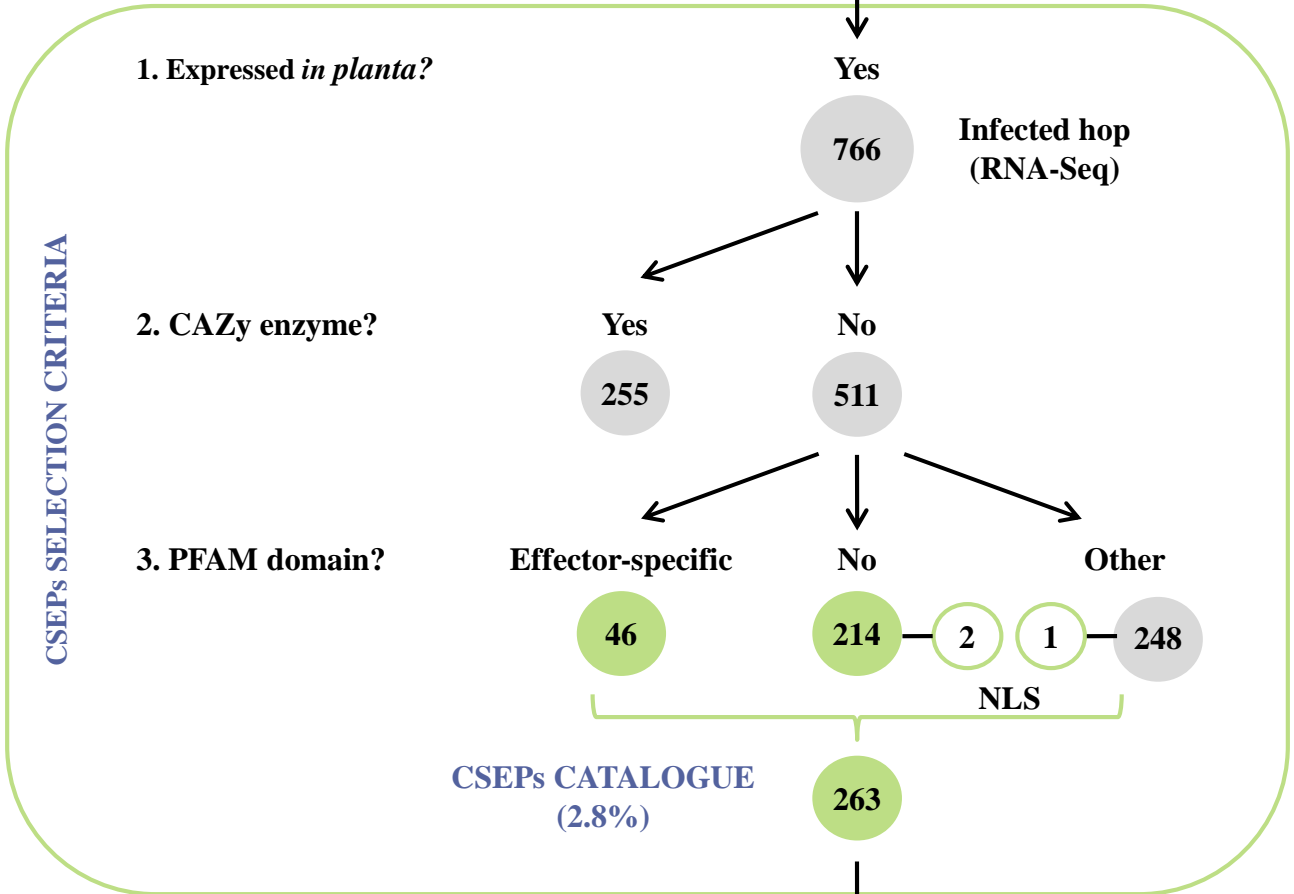
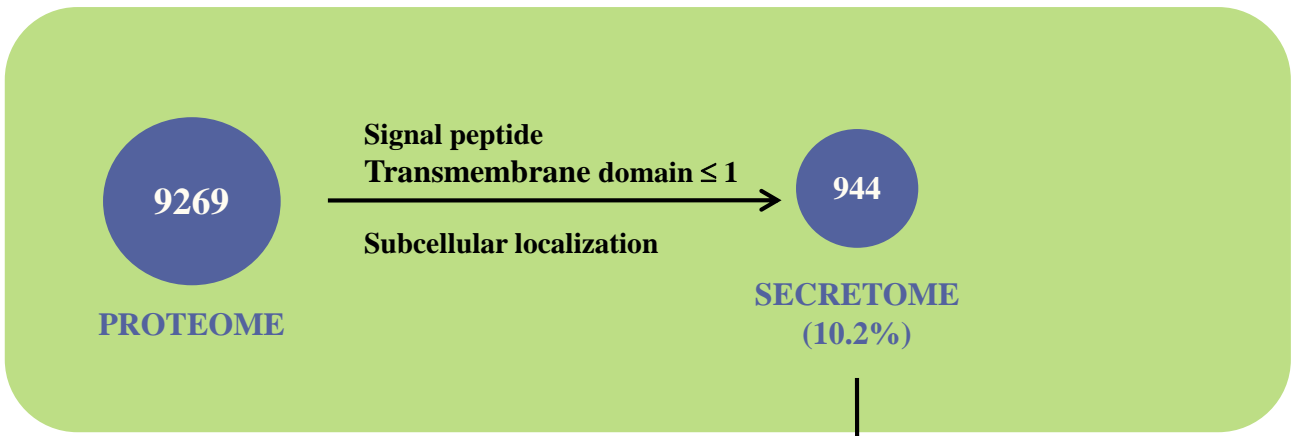
987 Table S8. List of primers used in this study. ^a, oligonucleotide designed according to template [123];
988 ^b, oligonucleotide that amplifies the promoter region of the target gene; ^c, oligonucleotide that
989 amplifies the terminator region of the target gene; ^d, oligonucleotide that amplifies the target gene for
990 knockout (KO) selection; ^e, oligonucleotide that amplifies genomic and vector sequences for KO
991 selection; ^f, *V. nonalfalfae* lethal pathotype-specific marker [97].

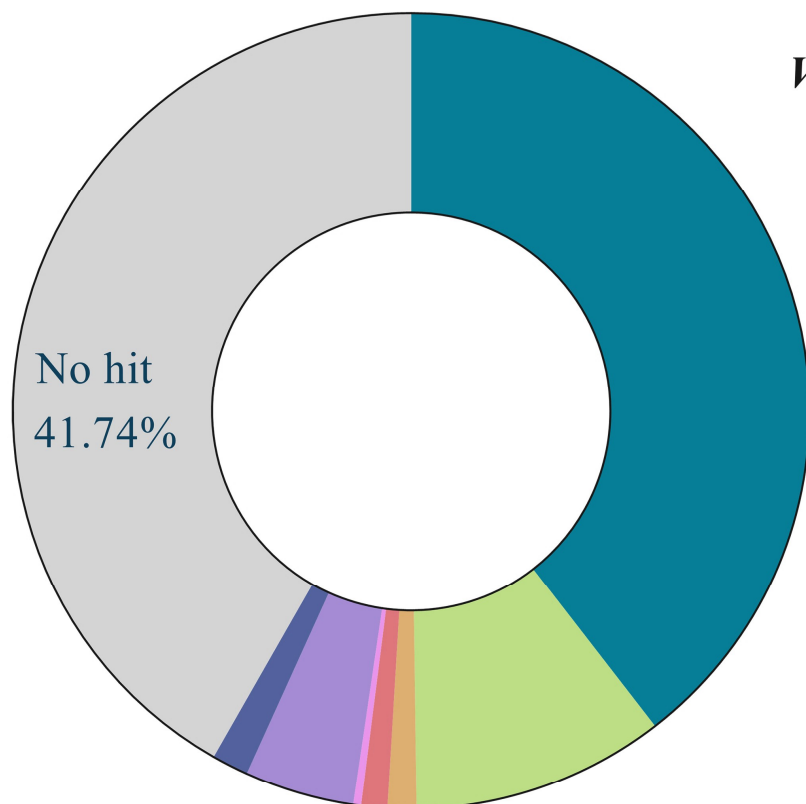
992 Additional file 2. A figure in PDF format. Enrichment of carbohydrate metabolic processes and
993 peptidase activity in the predicted *V. nonalfalfae* secretome compared to proteome. GO terms for
994 biological process (A) and molecular function (B) are presented at GO level 4. Relative abundance of
995 gene ontology (GO) terms determined by Blast2GO is expressed in percentages of predicted fungal
996 secretome and proteome, respectively.

997 Additional file 3. A figure in PDF format. A heatmap displaying the expression patterns of *V.*
998 *nonalfalfae* genes during infection of susceptible 'Celeia' and resistant hop 'Wye Target'. Fungal
999 transcripts were first identified by mapping of reads with at least 90% sequence identity and 90%
1000 sequence coverage to the *V. nonalfalfae* reference genome [22] using CLC Workbench.
1001 Normalization by trimmed mean of M values (TMM) [129] was performed to eliminate composition
1002 biases between libraries. Read counts were converted into log₂-counts-per-million (logCPM) values
1003 and a cutoff of CPM >1 was chosen. Color scale bar represents the logCPM values, with darker red
1004 color meaning higher expression values.

1005 Additional file 4. A figure in PDF format. Some *V. nonalfalfae* CSEPs deletion mutants exhibit
1006 unaffected pathogenicity. Relative area under the disease progress curve (rAUDPC) is presented for
1007 the three *V. nonalfalfae* deletion mutants (each in four replicates) and the wild type fungus. Depicted

1008 are mean values \pm SEM (n=10). Analysis of variance was first performed by Levene's test, followed
1009 by Dunnett's test to compare each treatment (knockout) with a single control (wild type); however,
1010 no statistical differences were found at α level of 5%.





V. nonalfalae secretome: 944 proteins

Metabolism (39.51%)

Polysaccharide metabolism and transport	91
Carbohydrate metabolism and transport	62
Redox	38
Secondary metabolism	27
Transferases	8
Coenzyme metabolism and transport	5
Cell envelope metabolism and transport	4
Nitrogen metabolism and transport	4
Amino acids metabolism and transport	1
Nucleotide metabolism and transport	2
E- transfer	1
Other enzymes	131

Processes IC (10.27%)

Proteases	72
Ion metabolism and transport	17
Phospholipid metabolism and transport	7
Transport	1

Processes EC (1.17%)

Cell adhesion	9
Toxins/defense	1
Blood clotting	1

Information (1.06%)

DNA replication/repair	9
RNA processing	1

Regulation (0.32%)

DNA-binding	2
Signal transduction	1

General (4.45%)

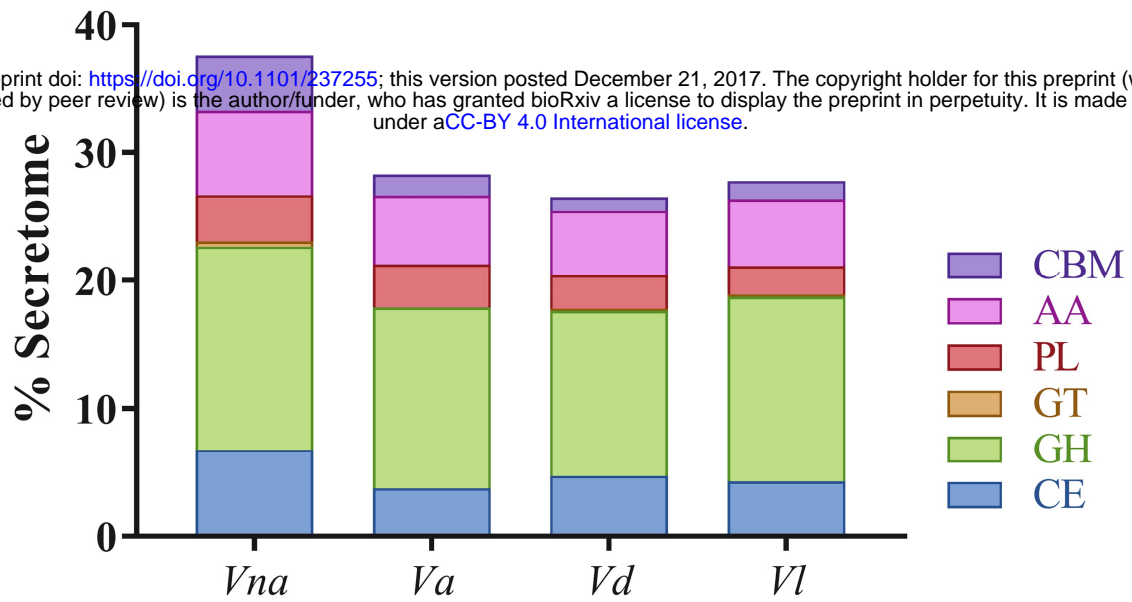
Small molecule binding	34
Protein interaction	3
General	3
Ligand binding	2

Other (1.48%)

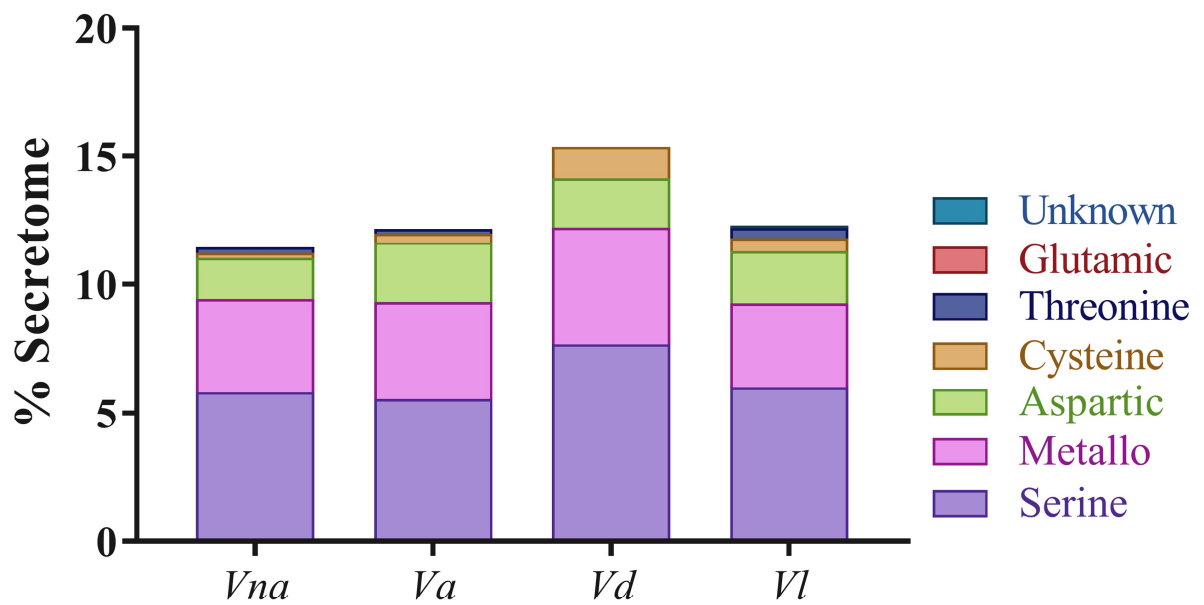
Unknown function	11
Viral proteins	2

(A)

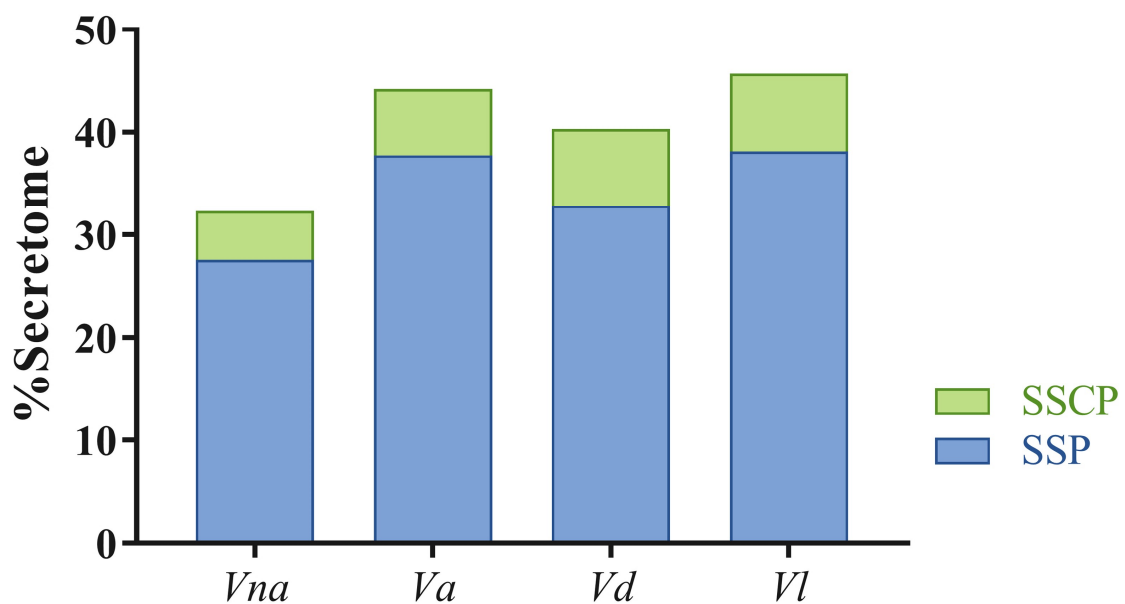
bioRxiv preprint doi: <https://doi.org/10.1101/237255>; this version posted December 21, 2017. The copyright holder for this preprint (which was not certified by peer review) is the author/funder, who has granted bioRxiv a license to display the preprint in perpetuity. It is made available under aCC-BY 4.0 International license.

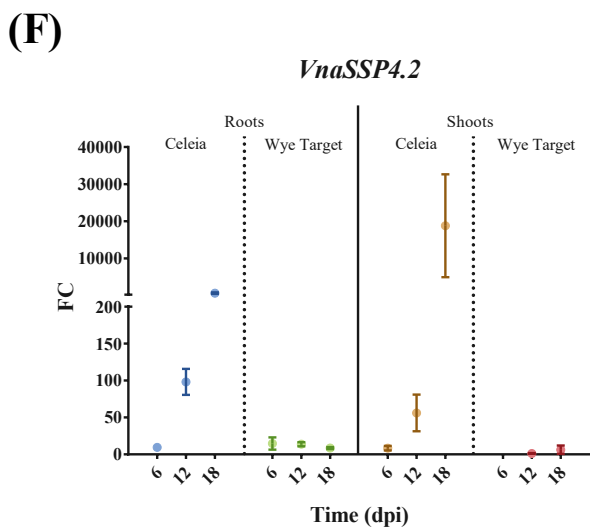
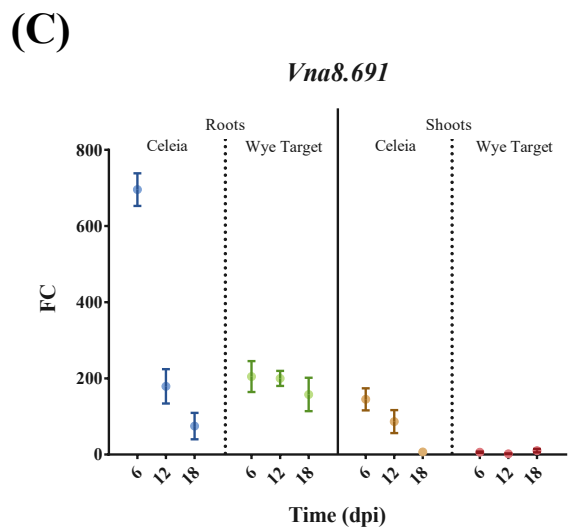
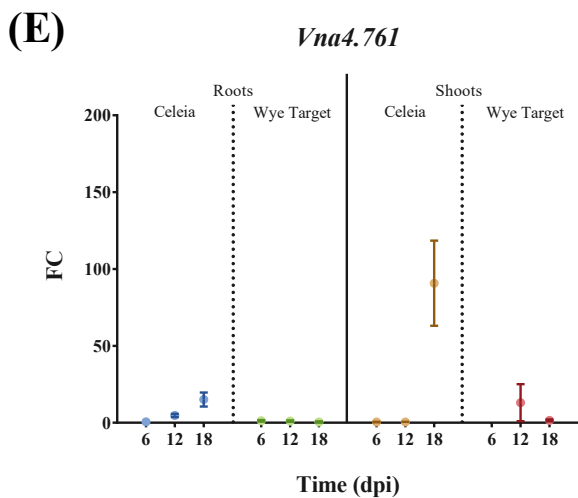
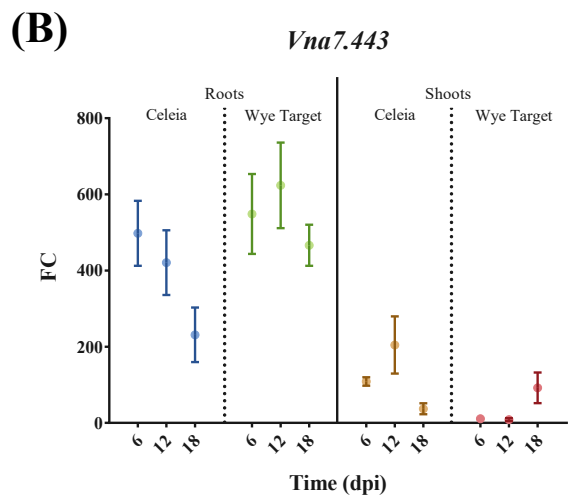
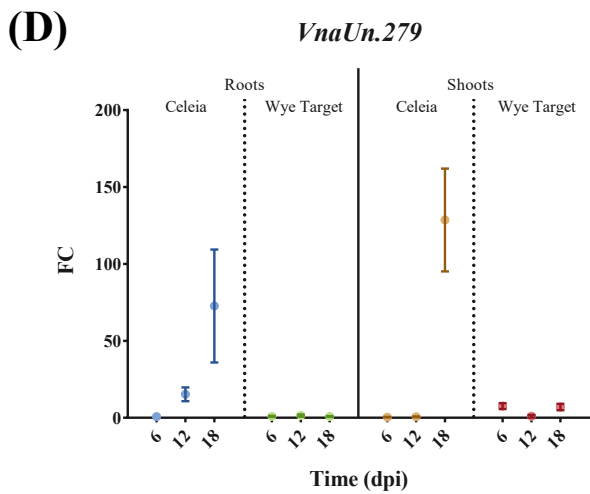
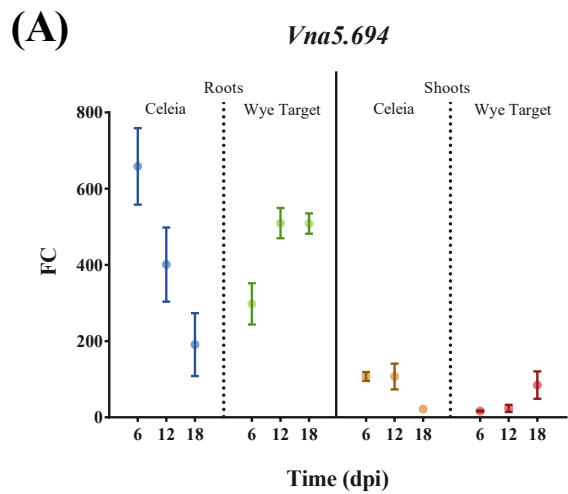


(B)



(C)

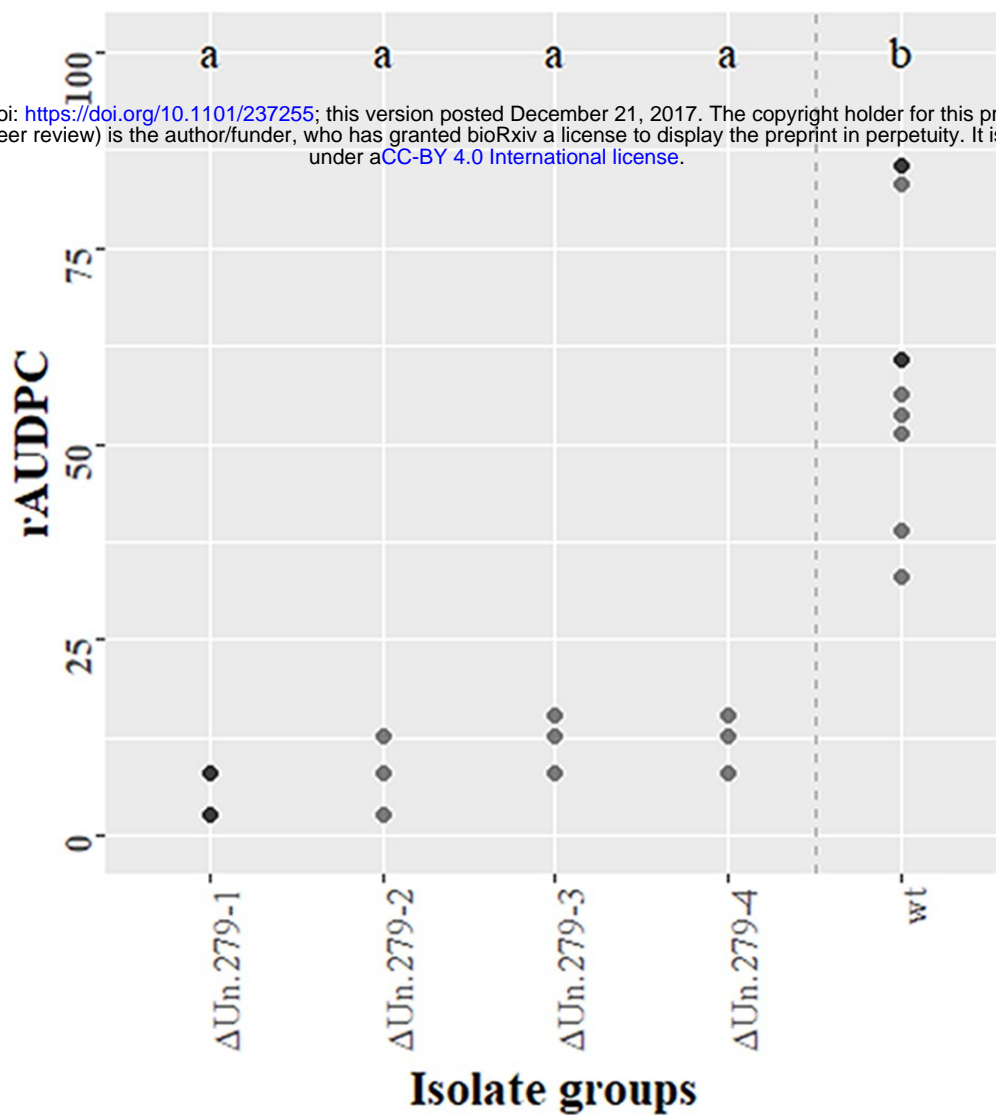






A

bioRxiv preprint doi: <https://doi.org/10.1101/237255>; this version posted December 21, 2017. The copyright holder for this preprint (which was not certified by peer review) is the author/funder, who has granted bioRxiv a license to display the preprint in perpetuity. It is made available under aCC-BY 4.0 International license.



B

